

1 **A new habitat map of the Lena Delta in Arctic Siberia**  
2 **based on field and remote sensing datasets**

3 Simeon Lisovski<sup>1,\*</sup>, Alexandra Runge<sup>2,\*</sup>, Iuliia Shevtsova<sup>1</sup>, Nele Landgraf<sup>3</sup>, Anne Morgenstern<sup>2</sup>,  
4 Ronald Reagan Okoth<sup>1,4</sup>, Matthias Fuchs<sup>2</sup>, Nikolay Lashchinskiy<sup>5,6</sup>, Carl Stadie<sup>2,7</sup>, Alison  
5 Beamish<sup>8</sup>, Ulrike Herzs Schuh<sup>1,9,10</sup>, Guido Grosse<sup>1,11</sup>, Birgit Heim<sup>1</sup>

6

7 \* Both authors contributed equally

8 <sup>1</sup> Alfred Wegener Institute Helmholtz Centre for Polar and Marine Research, Polar Terrestrial  
9 Environmental Systems, 14473 Potsdam, Germany

10 <sup>2</sup> Alfred Wegener Institute Helmholtz Centre for Polar and Marine Research, Permafrost Research, 14473  
11 Potsdam, Germany

12 <sup>3</sup> Humboldt University, Department of Geosciences, 12489 Berlin, Germany

13 <sup>4</sup> Julius-Maximilians Universität Würzburg, Institute of Geography and Geology, Oswald-Külpe-Weg 86,  
14 97074 Würzburg, Germany

15 <sup>5</sup> Central Siberian Botanical Garden, Siberian Branch, Russian Academy of Sciences, Novosibirsk,  
16 630090 Russia

17 <sup>6</sup> Trofimuk Institute of Petroleum Geology and Geophysics, Siberian Branch, Russian Academy of  
18 Sciences, Novosibirsk, 630090 Russia

19 <sup>7</sup> University of Greifswald, Institute for Geography and Geology, Germany (current address: University of  
20 Copenhagen, Department of Earth Science and Nature Management, Denmark)

21 <sup>8</sup> GFZ German Research Centre for Geosciences, Helmholtz Centre Potsdam.

22 <sup>9</sup> University of Potsdam, Institute of Environmental Sciences & Geography, Karl-Liebknecht-Str. 24-25,  
23 14476 Potsdam, Germany

24 <sup>10</sup> University of Potsdam, Institute of Biochemistry and Biology, Karl-Liebknecht-Str. 24-25, 14476  
25 Potsdam, Germany

26 <sup>11</sup> University of Potsdam, Institute of Geosciences, Karl-Liebknecht-Str. 24-25, 14476 Potsdam, Germany

27 Correspondence to: Simeon Lisovski ([Simeon.Lisovski@awi.de](mailto:Simeon.Lisovski@awi.de)), Alexandra Runge  
28 ([alexandra.runge@gfz-potsdam.de](mailto:alexandra.runge@gfz-potsdam.de)), Birgit Heim ([birgit.heim@awi.de](mailto:birgit.heim@awi.de))

29

Deleted: (Simeon.Lisovski@awi.de)

31 **Abstract.** The Lena Delta is the largest river delta in the Arctic (about 30 000 km<sup>2</sup>) and prone to  
32 rapid changes due to climate warming, associated cryosphere loss and ecological shifts. The delta is  
33 characterized by ice-rich permafrost landscapes and consists of geologically and geomorphologically  
34 diverse terraces covered with tundra vegetation and of active floodplains, featuring approximately 6  
35 500 km of channels and over 30 000 lakes. Because of its broad landscape and habitat diversity the  
36 delta is a biodiversity hotspot with high numbers of nesting and breeding migratory birds, fish,  
37 caribou and other mammals and was designated a State Nature Reserve in 1995. Characterizing  
38 plant composition, above ground biomass and application of field spectroscopy was a major focus of  
39 a 2018 expedition to the delta. These field data collections were linked to Sentinel-2 satellite data to  
40 upscale local patterns in land cover and associated habitats to the entire delta. Here, we describe  
41 multiple field datasets collected in the Lena Delta during summer 2018 including foliage projective  
42 cover (Shevtsova et al., 2021a), above ground biomass (Shevtsova et al., 2021b), and hyperspectral  
43 field measurements (Runge et al., 2022, <https://doi.pangaea.de/10.1594/PANGAEA.945982>). We  
44 further describe a detailed Sentinel-2 satellite image-based classification of [habitats](#) for the central  
45 Lena Delta (Landgraf et al., 2022), an upscaled classification for the entire Lena Delta (Lisovski et  
46 al., 2022), as well as a synthesis product for disturbance regimes (Heim and Lisovski, 2023,  
47 <https://doi.org/10.5281/zenodo.7575691>) in the delta that is based on the classification, the  
48 described datasets, and field expertise. We present context and detailed methods of these openly  
49 available datasets and show how [their combined use](#) can improve our understanding of the rapidly  
50 changing Arctic tundra system. The new Lena Delta habitat [classification](#) represents a first baseline  
51 against which future observations can be compared. [The](#) link between such detailed habitat  
52 [classifications](#) and disturbance [regime](#) may provide a better understanding of how Arctic lowland  
53 landscapes will respond to climate change and how this will impact land surface processes.

Deleted: habitat types

Deleted: they

Deleted: distribution dataset

Deleted: With the

Deleted: type

Deleted: regimes future upscaling efforts

54

# 61 1 Introduction

62 Global warming has profound impacts on the polar regions (Serreze and Barry, 2011; Overland et  
63 al., 2019). Rapidly increasing temperatures and changing precipitation regimes result in declining  
64 sea ice, warming and thawing of permafrost, more frequent tundra fires, and changes in vegetation  
65 (e.g., Biskaborn et al., 2019; Hu et al., 2015; Mauclet et al., 2022; Box et al., 2019; Amap, 2021).  
66 The Arctic tundra biome, which is normally characterized by harsh living conditions and nutrient-  
67 deficiency, has experienced rapid phenological shifts, such as earlier green-up in spring, which is  
68 also associated with increasing shrubification rates (Mekonnen et al., 2021). Shifts in plant  
69 communities are also driven by changing nutrient availability in permafrost soils (Mekonnen et al.,  
70 2021; Mauclet et al., 2022), affecting the net primary productivity of tundra ecosystems.

71 Satellite-derived remote sensing can provide large-scale assessments of Arctic vegetation cover and  
72 changes therein (Bartsch et al., 2016). For example, the Circumpolar Arctic Vegetation Map (CAVM)  
73 project, from the Conservation of Arctic Flora and Fauna working group (CAFF), provided a first  
74 panarctic vegetation composition map based on Advanced Very-High Resolution Radiometer  
75 (AVHRR) false-color infrared (CIR) composites at a 1:4 million map scale (Walker, 1998; Raynolds  
76 et al., 2019). Later, higher resolution land cover maps became available across all spatial scales  
77 from national and international efforts such as the NASA Arctic-Boreal Vulnerability Experiment  
78 (ABoVE) providing open-source data collections from boreal and arctic regions (ABoVE Science  
79 Definition Team, 2014) specifically for Alaska, Canada, Northern Europe, and Western Siberia,  
80 providing a better bridge to field measurements. Such products greatly assist in monitoring and  
81 upscaling of patterns and dynamics of soil properties, land-atmosphere fluxes, ecosystem states,  
82 and changes therein (e.g., Walker, 1998; Beamish et al., 2020; Berner et al., 2020; Sweeney et al.,  
83 2022; Macander et al., 2022; Endsley et al., 2022). For selected Eastern Siberian tundra regions,  
84 land cover maps have been produced (e.g., Veremeeva and Gubin, 2009; Bartsch et al., 2019;  
85 Schneider et al., 2009), including the Lena Delta (Bartsch et al., 2019; Schneider et al., 2009).

86 Arctic river deltas represent distinct and vulnerable geomorphological and ecological regions at the  
87 marine-terrestrial boundary. River deltas have been studied intensively to better understand land  
88 cover and vegetation compositions (Jorgenson, 2000; Schneider et al., 2009; Frost et al., 2020;  
89 Bartsch et al., 2020), carbon pools and fluxes (Bartlett et al., 1992; Schneider et al., 2009; Sachs et  
90 al., 2008; Rossger et al., 2022), and land cover change caused by climate change impacts  
91 (Jorgenson, 2000; Pizaric et al., 2011; Lantz et al., 2015; Nitze and Grosse, 2016; Vulis et al., 2021;  
92 Juhls et al., 2021). With diverse habitats, Arctic river deltas are biodiversity hotspots (Gilg et al.,  
93 2000), but at the same time are prone to rapid changes (Walker, 1998; Overeem et al., 2022). Arctic

94 deltas are affected by permafrost thaw (e.g., Pizaric et al., 2011; Nitze and Grosse, 2016; Vulis et  
95 al., 2021), sea ice loss (Overeem et al., 2022), and increased sediment transport and organic load  
96 during spring floods (Piliouras and Rowland, 2020; Juhls et al., 2021). Arctic river deltas are very  
97 dynamic systems and high-resolution habitat information from these biodiversity hotspots is needed  
98 to assess and predict changes and implications of Arctic warming.

99 The Lena Delta is the largest Arctic river delta representing a typical lake-rich lowland permafrost  
100 landscape (Grigoriev, 1993). Over the past decades, the central Lena Delta became a place of  
101 intensive international research. In addition to long-term permafrost monitoring at the Research  
102 Station Samoylov Island (Hubberten et al., 2006; Boike et al., 2019), extensive records on  
103 meteorology, soil and ecosystem characteristics (Zibulski et al., 2016; Boike et al., 2019; Boike et al.,  
104 2008), hydrology (Fedorova et al., 2015), and greenhouse gas fluxes (Rossgger et al., 2022; Holl et  
105 al., 2019) are available, setting an important benchmark for further assessments of changes in an  
106 Arctic river delta. During the summer season of 2018, an extensive field campaign to the Lena Delta  
107 led to an unprecedented amount of field datasets including vegetation cover recordings, above  
108 ground biomass estimates, and spectral characterisation of the different vegetation/land cover units.  
109 These in situ datasets provide improved thematic detail allowing the development of habitat  
110 classifications. In 2009, Schneider et al. (2009) developed the first land cover classification map for  
111 the entire delta at 30 m spatial resolution based on Landsat-7 ETM+ satellite summer images from  
112 2000 and 2001 to quantify delta-wide methane emissions. The availability of Sentinel-2 (S-2)  
113 Multispectral Instrument (MSI) data from two orbiting satellite missions since 2016 and 2017 provide  
114 high quality multispectral satellite data with a higher spatial resolution in the Visible and Near  
115 Infrared wavelength of up to 10 m, and of 20 m in the Red Edge and the Short-Wave Infrared  
116 wavelength regions (Drusch et al., 2012, ESA 2015). Together with the extensive ground  
117 observations from the Lena Delta in 2018 this enables an updated classification, using the higher  
118 resolution, S-2 images and improved thematic detail.

119 In the following study, field datasets as well as derived multispectral satellite images from the  
120 summer season 2018 for the Lena Delta were used to provide 1) an updated data-driven framework  
121 for plant communities and associated habitat classes in the Lena Delta, 2) a high-resolution habitat  
122 mapping product for the entire delta, and 3) a disturbance regime map linked to habitat classes.  
123 These datasets enhance our understanding of the Lena Delta system and will build a baseline and  
124 framework for future spatio-temporal analysis of more detailed processes and changes within this  
125 highly sensitive ecosystem.

Deleted: last

Deleted: has been

Deleted: projects

Deleted: increase

Deleted: datasets collected within

Deleted: higher resolution Sentinel-2 (S-2, 10 to 20 m pixel...

Deleted: )

Deleted: based on extensive ground observations.

Deleted: and

Deleted: Earth Observation products based on

Deleted: , S-2

Deleted: data

Deleted: as an example for the application of such an habitat map ...

Deleted: an upscaling of information on

Deleted: regimes and links

Deleted: types. Integrating these

Deleted: enhances

## 145 2 Study Area

146 The Lena Delta is located in northeastern Siberia's continuous permafrost zone between 72° and  
147 74°N and 123° to 130°E (Figure 1). With an area of about 30 000 km<sup>2</sup>, it is the largest delta in the  
148 Arctic and one of the largest in the world (Walker, 1998; Schneider et al., 2009). It is surrounded by  
149 the Laptev Sea to the west, north, and east, and the Chekanovsky and Kharaulakh mountain ranges  
150 border it to the south. The delta is characterized by numerous river channels and more than 1500  
151 islands with a diverse geologic history (Grigoriev, 1993). Morphologically, the delta can be divided  
152 into three distinct geomorphological main terraces (Grigoriev, 1993; Schwamborn et al., 2002). The  
153 first main terrace, which comprises the Holocene fluvial terraces and the active floodplains, is the  
154 youngest and most active part of the delta (Schwamborn et al., 2023), and covers most of the east-  
155 northeastern areas as well as the southern and southwestern-most parts. This main terrace  
156 predominantly consists of ice wedge-polygonal tundra (Nitzbon et al., 2020) as well as of barren and  
157 vegetated floodplain areas (e.g., Rossger et al., 2022). The second main terrace, located in the  
158 northwestern part, contains mostly sandy, comparably well-drained soils with low ground-ice content  
159 (Schwamborn et al., 2002; Ulrich et al., 2009). Large, mostly north-to-south oriented lakes and  
160 depressions are abundant in this area (Morgenstern et al., 2008). The third and oldest main terrace  
161 consists mainly of remnants of a Late Pleistocene accumulation plain with ice- and organic-rich  
162 sediments (so-called Yedoma deposits) and is characterized by polygonal tundra with large ice  
163 wedges, deep thermokarst lake basins, and thermo-erosional valleys (Morgenstern et al., 2011;  
164 Morgenstern et al., 2021). The third terrace is found on islands in the southern delta region  
165 (Schirrmeister et al., 2003; Schirrmeister et al., 2011). Permafrost in the area has a thickness of  
166 about 500–600 m (Romanovskii and Hubberten, 2001). The active layer depth, i.e., the seasonally  
167 thawing upper soil layer, on the first terrace is usually in the range of 30 to 50 cm and 80 to 120 cm  
168 on the floodplains (Boike et al., 2019). The larger region is characterized by an Arctic continental  
169 climate with low mean annual air temperatures of –13 °C, a mean temperature in January of –32 °C,  
170 and a mean temperature in July of 6.5 °C. The mean annual precipitation is low and amounts to  
171 about 190 mm (World Weather Information Service).

172 As part of past Russian-German expeditions to the Lena Delta, most research during the last two  
173 decades has been carried out on the islands of Samoylov and Kurungnakh in the central delta  
174 (Figure 1). Samoylov Island (72°22' N, 126°29' E) covers an area of about 5 km<sup>2</sup> and is  
175 representative of the first terrace together with an active floodplain (Boike et al., 2019; Boike et al.,  
176 2008). The vegetation and soil types are diverse at local scales due to high lateral variability of the  
177 polygonal microrelief consisting of drier polygon rims, and moist to wet polygonal depressions and  
178 troughs (Nitzbon et al., 2020; Kienast and Tsherkasova, 2001). In contrast, Kurungnakh Island is

179 mainly composed of late Pleistocene Yedoma deposits that belong to the third delta terrace  
180 (Grigoriev, 1993) with elevation up to 55 m above sea level (m a.s.l.) (Morgenstern et al., 2013).  
181 Holocene cover deposits and peat-rich permafrost soils are distributed across the surface of the third  
182 Lena River terrace and especially concentrated in the deep thermokarst basins called “alases”.  
183 Alases are important landscape-forming features of the ice-rich Yedoma permafrost zone, which are  
184 mainly caused by extensive melting of excess ground ice in the underlying permafrost (Van  
185 Everdingen, 1998).

186

### 187 3 Datasets and methods

188 Several new datasets are presented for the Lena Delta that are spatially and thematically connected  
189 and support vegetation, habitat, and land cover applications for this region (Figure 1).

Deleted: Here,

Deleted: and an upscaling application

190 Two datasets feature field-measured vegetation data, providing information on foliage projective  
191 cover (Dataset 1) and above ground biomass (Dataset 2) recorded in the central Lena Delta in  
192 summer 2018 across 26 selected vegetation plot sites (supplementary table S1, S2). The field plots  
193 of 30 x 30 m (900 m<sup>2</sup>) were chosen to be representative for typical vegetation communities (vascular  
194 plants, moss and lichen cover) as largely homogenous sites representative for the surrounding area.  
195 In addition, a total of 28 in-situ, canopy-level hyperspectral field measurements were acquired in 30  
196 x 30 m plots with homogeneous vegetation or barren to partially vegetated areas (spectral  
197 reflectance field measurements; Dataset 3). Of the 28 hyperspectral measurements, 15 were  
198 conducted at the vegetation plot sites of Datasets 1,2 three measurements were repeat  
199 measurements to capture vegetation senescence, and at 10 spectrometry plots we conducted  
200 hyperspectral field measurements without floristic inventories but with detailed plot documentation.

Deleted: ,

201 Based on expert knowledge, we defined representative habitat classes and identified homogeneous  
202 regions within the central Lena Delta to train and apply a classifier using a S-2 satellite image from  
203 summer 2018 (Dataset 4). Due to the high reliability of the central Lena Delta vegetation  
204 classification and positive evaluation by field experts, we used this vegetation classification as a  
205 training dataset for a robust classifier that was subsequently applied to a S-2 image mosaic for the  
206 entire Lena Delta for 2018 to develop a new Lena Delta habitat map (Dataset 5).

Deleted: land cover

Deleted: vegetation

Deleted: Sentinel

Deleted: (S2)

Deleted: accuracy

Deleted: Sentinel

207 Finally, using the habitat classes, probability maps for exposed sandbars and water distribution, and  
208 information from the in-situ dataset (Datasets 1 & 2), we extrapolated a classification of disturbance  
209 regimes across the delta (Dataset 6) as an application example for the habitat classes.

Deleted: empirical

220 **3.1 Foliage projective cover (Dataset 1)**

221 A detailed description of plant composition for the 26 vegetation plots of the 2018 expedition to the  
222 Lena Delta was compiled (see supplementary table S1, S2, S3). Prior to the field work, the  
223 approximate site locations were defined for establishing representative vegetation plots based on  
224 field knowledge and [evaluation of Landsat and Sentinel-2 satellite imagery](#). The aim was to cover  
225 representative vegetation communities of the central delta. [There are vegetation communities with](#)  
226 [large area coverage that show high homogeneity within larger areas \(10s of meters\). Therefore, at](#)  
227 each site location, we defined a 30 x 30 m square plot with a homogeneous [or repetitive](#) vegetation  
228 [composition](#) that was also representative of the wider land surface serving as an Elementary  
229 Sampling Unit (ESU). [ESUs](#) according to the Committee on Earth Observing Satellites Working  
230 Group on Calibration and Validation ([Duncanson et al., 2021](#)) [serve as spatial training and](#)  
231 [validation units representative for the land surface for quantitative and qualitative remote](#)  
232 [sensing operations](#). In case of [more patchy and heterogeneous](#) vegetation [structure](#) we [selected](#) 30  
233 x 30 m squares [embedded](#) in a minimum of 50 x 50 m square of the same [vegetation composition](#).  
234 [The detailed floristic composition was recorded](#) around the plot [center](#) in [four successive](#) rings of 50  
235 cm [diameter](#). In addition, the vegetation plot was mapped in detail from above with one Red-Green-  
236 Blue (RGB) and one Red-Green-Near Infrared (RGNIR) [MAPIR](#) camera using telescope stick-based  
237 field photography. [The projective vegetation cover](#) was recorded in at least three subplots (2 m x 2  
238 m) [within](#) the plot. If the [vegetation cover](#) was [highly](#) homogenous, three subplots were established.  
239 In the case of [moisture differences, e.g. in](#) polygonal tundra with dry rims and moist to wet  
240 depressions, [we](#) established [higher numbers of subplots capturing moist as well as dry patches](#)  
241 (see, Figure 2 & 3 describing the concept). We compiled the floristic composition to foliage projective  
242 cover by plant taxa on each 2 x 2 m subplot for the different canopy levels and [extrapolated for](#) the  
243 30 m x 30 m plot. [We used the RGB and NIR field photos to make an estimate on the share of moist](#)  
244 [and dry surface area to calculate an averaged projective vegetation cover. The ring survey data was](#)  
245 [not included in the plot average](#). The dataset of percentage foliage projective cover per vegetation  
246 plot is published in PANGAEA ([Shevtsova et al., 2021a](#),  
247 <https://doi.pangaea.de/10.1594/PANGAEA.935875>).

248 **3.2 Above ground plant biomass (Dataset 2)**

249 Above-ground biomass (ABG) was sampled in the field in 25 of the 26 vegetation plots in 2018 (see  
250 supplementary table S1, S2, S3). Within each 2 x 2 m subplot a 0.5 m x 0.5 m representative plot

Deleted: At

Deleted: plot centre in a

Deleted: type

Deleted: )

Deleted: patchier

Deleted: ,

Deleted: were careful that the

Deleted: were set

Deleted: type

Deleted: First, the projective vegetation cover

Deleted: centre was recorded

Deleted: width from the plot centre

Deleted: Detailed floristic composition

Deleted: per ground cover vegetation type inside

Deleted: ground

Deleted: , only

Deleted: more diverse vegetation, for example

Deleted: more subplots were

Deleted: upscaled to

Deleted: using

Deleted: photo maps.

Deleted: .

Deleted: selected

274 was selected for ABG sampling. AGB sampling for moss and lichens was conducted within 0.1 m x  
275 0.1 m subplots inside the 0.5 m x 0.5 m subplots.

276 In total, 174 fresh AGB samples were collected and weighed in the field or subsequently at the  
277 Samoylov research station. AGB samples with a weight exceeding 15 g were subsampled. The plant  
278 samples were then dried for two to four days in a warm dry place and finally oven-dried for ca. 24  
279 hours at a temperature of 60 °C before re-weighing. All AGB assessments per plant community type  
280 were upscaled to the 30 m x 30 m plot in g/m<sup>2</sup> using the [foliage projective cover data](#). The dataset of  
281 AGB per vegetation plot has been published in PANGAEA (Shevtsova et al., 2021b,  
282 <https://doi.pangaea.de/10.1594/PANGAEA.935923>).

Deleted: field photo maps.

### 283 3.3 Hyperspectral field measurements (Dataset 3)

284 Hyperspectral field measurements were conducted in the central Lena Delta in August 2018 with the  
285 aim to collect surface reflectance spectra of different homogeneous land cover units across a variety  
286 of delta land surfaces [and vegetation composition](#). In total, we collected 28 hyperspectral field  
287 measurements in homogeneous 30 x 30 m spectrometry plots ([Table S5](#)), with 15 of them equalling  
288 the vegetation plots across Samoylov and Kurungnakh islands (see Dataset 1 & 2 *and*  
289 *supplementary table S4*), three as repeat measurements at the end of August to capture the change  
290 in spectral signature during senescence since the beginning of August and the remaining 10 field-  
291 spectroscopy plots focusing on non-vegetated areas such as sandy parts of the floodplain. We  
292 conducted the field-spectroscopy measurements with a Spectral Evolution SR-2500 field  
293 spectrometer with a 1.5 m Fiber Optic Cable. The instrument was calibrated to spectral radiance  
294 within a wavelength range of 350 to 2500 nm. Within the 30 x 30 m homogeneous spectrometry  
295 plots we acquired about 100 individual measurements, randomly scattered across the plot. Before  
296 and after each survey we conducted reference measurements by measuring the back reflected  
297 downwelling radiance from a Zenith Lite™ Diffuse Reflectance Target of 50% reflectivity to normalize  
298 to surface reflectance percentages per wavelength. The averaged individual measurements of the  
299 reflectance of each spectrometry plot was published in the PANGAEA data repository (Runge et al.,  
300 2022, <https://doi.pangaea.de/10.1594/PANGAEA.945982>).

Deleted: .

Deleted: ,

### 301 3.4 Central Lena Delta habitat classification (Dataset 4)

#### 302 3.4.1 Habitat [classes](#)

303 Based on the vegetation plots (Dataset 1 & 2) and from field knowledge, different habitat [classes](#)  
304 characterized by distinct plant communities, moisture regimes and soil properties were defined. Non-

Deleted: Classes

Deleted: types

310 vegetated areas (e.g., sand) and water were added as additional classes using band thresholds  
311 (Table 1). During an iterative process within a S-2 based supervised classification, additional habitat  
312 classes that were not covered by the vegetation plots (Dataset 1 & 2) were added: i) The polygonal  
313 tundra complex could spectrally be separated into distinct classes related to different surface water  
314 abundance in the form of intra- and interpolygonal ponds, therefore, we implemented three different  
315 polygonal tundra complex classes, with up to 10%, 20%, 50% surface water cover respectively, and  
316 ii) one class of 'sparsely vegetated' representing the areas of transition zones between vegetated  
317 and barren. Table 1 provides details on habitat class descriptions and established methods to  
318 distinguish habitats.

#### 319 3.4.2 Satellite data processing

320 The central Lena Delta habitat classification is based on one high quality cloudless S-2 image from  
321 August 6 in 2018, representing the late summer. The S-2 top of atmosphere reflectance (TOA)  
322 image data was processed by the German Space Agency DLR (B. Pflug, oral communication, 2019)  
323 to bottom of atmosphere (BOA) surface reflectance using the newest version of the atmospheric  
324 correction processor Sen2Cor later released as ESA Sen2Cor in 2020. Atmospheric correction  
325 processing was performed with the default rural aerosol model. All spectral bands were resampled to  
326 the 10 m pixel resolution bands. The 60 m pixel resolution bands (B1, B9, B10) that support  
327 atmospheric correction, but are not optimal for land surface classification, were removed. We added  
328 the normalized difference vegetation index (NDVI; NIR-RED / NIR + RED) to the band collection.

#### 329 3.4.3 Central delta habitat classification

330 S-2 pixels from the 30 x 30 m FSUs (dataset 1, Shevtsova et al. 2021a), and additional polygons  
331 defined by expert knowledge, led to 8 626 training pixels (50% to train the classifier and 50% for  
332 validation) for the habitat classification (training points shown in Appendix A4 and are published in  
333 the Landgraf et al 2022a data collection). We tested several classifiers and different selected band  
334 combinations (spectral bands and NDVI). Water (transparent to turbid) and sandbanks were omitted  
335 in the classification processing by masking them as inactive using a band threshold. water mask was  
336 based on the NIR 10 m band 8 (NIR < 0.02) and the sand mask was based on the blue 10 m band 2  
337 (Blue > 0.07, Table 1). The classification was tuned to depict vegetation composition and was  
338 qualitatively assessed well known to the classification developers. Best results for the habitat  
339 classification were obtained using a random forest classification with a band combination of all S-2  
340 VIS, Red-Edge, NIR and SWIR bands, and the NDVI. The chosen classifier was able to distinguish  
341 between relevant classes (Table 1) and could even identify patchy spots of specific habitat classes.  
342 In addition to the defined water and sand classes, the final central Lena Delta classification contains

Deleted: the S

Deleted: types

Deleted: three

Deleted: vegetated

Deleted: as

Deleted: type

Deleted: 2A Level 2A

Deleted: Level-1C (

Deleted: ,

Deleted: Level-2A (

Deleted: ,

Deleted: The Sentinel

Deleted: vegetation plots,

Deleted: for

Deleted: .

Deleted: The classification was forced to express vegetation composition, biomass and moisture regimes. We omitted the water class

Deleted: the sandbank surfaces from

Deleted: method. The

Deleted: The final central Lena Delta habitat classification contains 12 classes (including water and barren/sand as distinct classes, see Table 1).

366 [10 habitat classes \(Table 1\)](#). The here defined central Lena Delta covers an area of 644.9 km<sup>2</sup> with a  
367 [55.2 % vegetation cover](#).  
368 [To assess the classification performance we applied a cross-validation on an independent random](#)  
369 [selection of the training pixels \(50 %\)](#). Based on a confusion matrix (supplementary table S5), the  
370 [classification accuracy was 96.78 %](#). However, this is partly due to strong autocorrelation resulting  
371 [from pixel selection within polygons](#). More importantly, the accuracy was qualitatively tuned and  
372 [evaluated based on ground-truthed knowledge of the development team](#). The published dataset of  
373 Landgraf et al. (2022, <https://doi.pangaea.de/10.1594/PANGAEA.945057>) provides the central Lena  
374 Delta habitat classification map, the ESUs and the polygons used to train the classifier. The training  
375 dataset includes data from 23 of the 26 vegetation plots (dataset 1). The dataset provides additional  
376 69 ESUs defined with expert knowledge gathered during several field expeditions to the Lena Delta,  
377 [labeled as pseudo ESUs for potential future investigations](#).

### 378 3.5 Lena Delta habitat classification (Dataset 5)

#### 379 3.5.1 Lena Delta habitat classes

380 In order to extend the habitat classification map to the entire Lena Delta (29873.7 km<sup>2</sup>), we included  
381 all the [habitat classes](#) covering the central Lena Delta (dataset 4, table 1). In addition, and based on  
382 expert knowledge [as well as](#) extensive visual satellite image investigations, we added [one](#) habitat  
383 [class](#) that is not present in the central Lena Delta: the second terrace in the northwest of the Lena  
384 Delta is lithologically and geomorphologically different from the other two terraces present in the  
385 central delta, and characterized by sandy substrates. In a hyperspectral CHRIS PROBA satellite-  
386 based [geomorphological](#) classification, Ulrich et al. (2009) described the second terrace featuring  
387 very dry elevated sandbanks, barren or poorly vegetated areas with isolated lichens, moss, herbs,  
388 dwarf shrubs or grasses (vegetation cover 0–60%, growth height: max. 20 cm, average active layer  
389 depth of 1 m on the upland plain with old, vegetation-arrested sand dunes). Based on photos taken  
390 [at few locations](#) in the field during past expeditions (see supplementary table S3) the habitat class  
391 shows well-drained areas dominated by sandy substrate and diverse, sparse vegetation cover; some  
392 areas are dominated by sedges, cotton grass and mosses with rare occurrences of lichens and  
393 dwarf shrubs, while some areas are dominated by the latter. Schneider et al. (2009) defined [the](#)  
394 [same](#) class as 'dry moss-, sedge- and dwarf shrub-dominated tundra (DMSD)'. We selected 35  
395 ESUs for this habitat class characterized by high SWIR reflectance (S-2 band 11) due to dry land  
396 surface conditions. The habitat [class](#) was named 'dwarf shrub - herb communities' and was added  
397 as an additional habitat class to the training data set.

398

Deleted: The chosen classifier was able to distinguish all relevant classes (Table 1) and was even able to identify patchy habitat spots. The result of

Deleted: indicated

Deleted: overall class accuracy of 96.78% . For the test,

Deleted: dataset, consisting of data points from the vegetation plots (Dataset 1, 2), was split in half and 4 313 pixel samples were used for a second run through the classification algorithm. The precision of each class was calculated with

Deleted: ).

Deleted: and

Deleted: Dataset 1, 2), as well as

Deleted: ,

Deleted: habitats

Deleted: delta (Dataset

Deleted: and

Deleted: an additional

Deleted: type

Deleted: land cover

Deleted: this

Deleted: type

421 3.5.2 Satellite data processing

422 The Lena Delta habitat classification was based on a S-2 mosaic (top of atmosphere (TOA)  
423 reflectance, Google Earth Engine Dataset) with images taken of the area between June 1 and  
424 September 15, 2018. The images (N = 1685, distributed across 15 S-2 tiles) were filtered to discard  
425 images with cloud cover above 20%. A cloud mask was applied to the remaining 262 images,  
426 masking pixels where the quality band 'QA60' indicates clouds (band 10) or cirrus (band 11). All  
427 spectral bands with 20 m resolution were resampled to match the 10 m resolution bands. Next, NDVI  
428 was computed (see 3.4) for each image and one high-quality mosaic of all images based on the  
429 maximum NDVI value per pixel was produced representing a snapshot of the peak summer  
430 vegetation period. Using the median NIR band values across the 262 cloud-masked images, we  
431 classified water with a threshold of  $< 0.07$  reflectance. The remaining non-vegetated areas defined  
432 by a threshold of  $NDVI < 0.4$  were classified as barren/sand. The water- and sand-masked image  
433 mosaics were then used in the classification pipeline with the following bands: B2 (blue), B3 (green),  
434 B4 (red), B5 (red edge 1), B6 (red edge 2), B7 (red edge 3), B8 (NIR), B11 (SWIR 1), B12 (SWIR 2),  
435 and NDVI.

436 3.5.3 Lena Delta Habitat classification

437 From the central Lena Delta habitat classification (dataset 4) we sampled 7 500 random pixels to  
438 train a random forest classifier (smileRandomForest in Google Earth Engine). In addition we added  
439 35 pixels from the ESUs selected within the 'dwarf shrub - herb communities' of the north-western  
440 Lena Delta. Unfortunately, no vegetation recording/monitoring schemes exist outside the central  
441 Lena Delta. Therefore, independent validation of the classification across the Delta is not possible.  
442 Similar to the validation of the central Lena Delta habitat classification, the results were carefully  
443 checked with expert knowledge from the central Delta and a few adjacent regions that are known to  
444 the developer team. Together with visual comparison of high resolution ESRI RGB satellite  
445 background images, we consider the results accurate. A formal validation based on another random  
446 sample of 5 000 points from the central Delta showed expected high accuracy of  $> 95\%$ .

447 Since the barren/sandy areas are highly dynamic with variable water levels mainly within (due to  
448 flooding in spring and decreasing river flow during the summer season) but also across years  
449 (discharge dynamics), we computed a sandbar probability map for the Lena Delta using cloud  
450 masked S-2 (TOA reflectance) images between April 1 and October 15 from 2015 to 2021 (6 026  
451 images). In each image, we labeled sandy pixels by  $NDVI < 0.4$  AND  $NDWI > 0.095$  AND  $NIR < 0.09$   
452 reflectance. Next, for each pixel in the Lena Delta, we computed the percentage of sandy pixels  
453 across all images resulting in a sand probability map. The training dataset (random 7500 points, plus

Deleted: Sentinel

Deleted: 1684

Deleted: Given the high accuracy and thorough validation of the ...

Deleted: Dataset

Deleted: used the result

Deleted: To this end,

Deleted: selected 7500 random points within the vegetated area of the central Lena Delta (labelled according to the underlying vegetation class of Dataset 4), plus...

Deleted: Visual inspection of experts found high accuracy in ...

Deleted: spatial distribution of

Deleted: classes across the delta. Formal validation was based on ...

Deleted: between the classification result and

Deleted: training dataset (Dataset 4). In addition, and since...

Deleted: Sentinel

Deleted: surface

Deleted: n =

Deleted: .

Deleted: image tiles

Deleted: labelled

Deleted: 9%

480 35 points with label 'dwarf shrubs - herb communities'), the habitat classification, and the sandbar  
481 probability map was published in the PANGAEA repository (Figure 5, Lisovski et al., 2022,  
482 <https://doi.pangaea.de/10.1594/PANGAEA.946407>).

### 483 3.6 Lena Delta disturbance regimes (Dataset 6)

484 [The Lena Delta experiences different disturbance regimes, mapped and described in dataset 6.](#)  
485 Mainly annual flooding, but also local rapid thaw processes on the land surface of the terraces with  
486 ice-rich permafrost, result in disturbance regimes forming distinct habitat [classes](#) (Table 2). The  
487 floodplains experience seasonal flooding as a regularly occurring disturbance in spring after ice-  
488 break up (the spring flood). Very high disturbance regimes due to the most intense scour, erosion  
489 and sedimentation result in barren sandbanks or in early-stage plant communities equalling the  
490 'sparsely vegetated' habitat class. [The classes](#) 'moist to wet sedge communities', 'wet sedge  
491 communities', 'moist equisetum and shrubs', 'dry shrub communities', 'dry grass to wet sedge  
492 communities' [represent](#) the mid to advanced successional stages on the floodplain [within areas of](#)  
493 high disturbance [that are also described as](#) shifting habitat [class](#) (Stanford et al., 2005; Driscoll and  
494 [Hauer, 2019](#)).

495 In contrast to [the high disturbance regimes on](#) the floodplain, habitats on the first, second and third  
496 delta terraces are less extensively disturbed (low disturbance). [In these areas](#) typical mature-state  
497 tundra plant communities [are able to develop](#): 'polygonal tundra complex', 'tussock tundra', and  
498 'dwarsh shrub herb communities'. However, locally, high disturbance occurs by rapid thaw  
499 processes of ice-rich permafrost [on the first and third delta terraces with habitats characterized by](#)  
500 mid to advanced-stage plant succession: 'moist to wet sedge communities', 'wet sedge  
501 communities', 'dry shrub communities', and 'dry grass to wet sedge' communities. Very high  
502 disturbance due to intense rapid thaw processes occurs at eroding cliffs and lake margins, in steep  
503 valleys and actively developing gullies resulting in barren surfaces with rims of sparsely vegetated  
504 transition zones. Given the link between plant communities and flooding as well as rapid thaw  
505 processes, we [characterized](#) the disturbance regimes for each habitat class (Table 2) and provide  
506 [mapped disturbance based on the habitat class of dataset 5 and the corresponding disturbance](#)  
507 [regime](#) for the entire Lena Delta (Figure 6, Heim and Lisovski, 2023,  
508 <https://doi.org/10.5281/zenodo.7575691>).

Deleted: types

Deleted: forms

Deleted: (

Deleted: regime) with

Deleted: types according to .

Deleted: ) allowing the development of the

Deleted: :

Deleted: (

Deleted: )

Deleted: :

Deleted: characterised

Deleted: an upscaling product in the form of a

Deleted: map

## 522 4 Results and Discussion

523 We deliver a detailed description and associated data products of the most prominent habitat  
524 classes in the largest Arctic river delta, the Lena Delta. Supported by ecological field data of plant  
525 composition, hyperspectral field measurements from the same sites, and regional expert knowledge  
526 collected over decades, we develop a high-resolution S-2 based habitat map for the entire delta. The  
527 compiled datasets, provide the necessary baseline for future investigations of the biochemical  
528 processes, ecological dynamics, and responses to global warming within the Arctic tundra system of  
529 the delta.

### 530 4.1 Habitat classes of the Lena Delta

531 Based on the floristic composition and biomass of the vegetation plots (Dataset 1, 2), the spectral  
532 properties from hyperspectral field measurements (Dataset 3) as well as expert knowledge, we  
533 defined 11 distinct habitat classes linked to different vegetation composition for the Lena Delta  
534 (Figure 4). The selected S-2 spectral bands and the derived NDVI values allow a separation of the  
535 habitat classes into two distinct groups (the first separation level between habitat classes in Figure  
536 4a, 1st hierarchical level). Three habitat classes ('wet sedge communities', 'moist Equisetum and  
537 shrub communities', 'dry grass to wet sedge communities') formed in areas of high disturbance by  
538 rapid thaw processes and regular flooding represent a distinct cluster with highest vegetation vitality  
539 (high NDVI), and separated from the more stable and mature tundra communities ('polygonal tundra  
540 complex', 'dry (tussock) tundra', and 'dry dwarf-shrub and herb communities'), and the other  
541 successional plant communities ('moist to wet sedge complex', 'dry low shrub communities' and  
542 'sparsely vegetated') all characterised by a lower NDVI range. The 'dry dwarf-shrub and herb  
543 communities' form a separate cluster with the least overlap with other habitat classes within the two-  
544 dimensional non-metric multidimensional scaling (NMDS) space (2nd hierarchical level, Figure 3a;  
545 Figure 4c) due to very low vegetation vitality and surface moisture (lowest NDVI, high red and SWIR  
546 reflectance). There are two remaining habitat classes on the 3rd and 4th hierarchical level, which are  
547 successional plant communities, the 'moist to wet sedge complex' and 'dry low shrub communities'.  
548 The separation on the 3rd and 4th hierarchical level is mainly driven by higher NDVI of these  
549 successional plant community classes in comparison with the mature state tundra plant communities  
550 with lower NDVI (Figure 4a-b). The 'dry grass to wet sedge communities' and the 'sparsely  
551 vegetated area' habitat class (not covered by vegetation plots but added during the classification  
552 process), show the largest overlap with the other habitat classes due to a high variability in  
553 vegetation cover, biomass and moisture. In general, the ordination method (Figure 4b) shows that  
554 distinct plant communities and the associated habitat classes are mostly separated by a biomass

Deleted: Combining

Deleted: as well as S-2 satellite data, allowed us to

Deleted: and analyses

Deleted: and S-2 satellite data,

Deleted: 3

Deleted: 1, Figure 3a

Deleted: types

Deleted: 2

Deleted: 3c

Deleted: 3a/

Deleted: type

Deleted: types

Deleted: 3b

568 gradient for which the NDVI is a good approximator. A further separation linked to potential spectral  
569 proxies for biomass exists with the far red-edge and NIR bands (B6,7,8) but is less distinct than the  
570 NDVI axis. Together with the SWIR (B11,12) the red (B4) and near red-edge (B5) bands, and less  
571 strongly the blue and green bands (B2,3), the results indicate a habitat class separation based on  
572 moisture, biomass and vegetation colour characteristics.

573 The vegetation plot selection was made in relation to the most typical habitats (e.g., Mueller-  
574 Bombois and Ellenberg, 1974). For 15 of the 26 vegetation plots, we collected and provided  
575 hyperspectral surface reflectance data (Runge et al., 2021). These measurements cover a variety of  
576 landscape units including Yedoma uplands, floodplains (vegetated and non-vegetated), drained  
577 thermokarst lake basins (old and recently drained), and areas covered by low shrub layers.  
578 Comparing the hyperspectral surface reflectance with multispectral S-2 data, we found  
579 commonalities in the discrimination of habitat classes along moisture gradients. Unfortunately, the  
580 hyperspectral field measurements do not cover the biomass gradient. Plot measurements with the  
581 field spectrometer are conducted with the hand-held instrument held at shoulder height, hence it was  
582 not possible to acquire field spectroscopy measurements in disturbed patches with tall shrubs or  
583 very sloped terrain. This highlights the difficulty in deriving high spectral resolution surface  
584 reflectance measurements representative of fine scale differences between Arctic tundra habitat  
585 classes if the plot properties become too challenging to measure.

Deleted: provide

586 In general, mature-state tundra plant communities have relatively similar spectral properties due to  
587 low vascular plant cover (e.g., Beamish et al., 2017). In addition, the tundra vegetation communities  
588 contain a wide range of accessory pigment composition (carotenoids and anthocyanins) that result in  
589 a very similar spectral response (Beamish et al., 2018). Only the highly disturbed communities such  
590 as wetlands or areas with tall shrubs are more spectrally distinct due to a high NIR reflectance  
591 plateau (Buchhorn et al., 2013). Since the hyperspectral field measurements provide a higher spatial  
592 resolution and thus also a measure of variability within areas of the same general habitat type, we  
593 consider the measurements valuable for applications that aim at analysing ecological and  
594 biochemical processes within distinct habitats in more detail.

Deleted: conditions

#### 595 4.2 Sentinel-2 based habitat classification

596 Based on the identified habitat classes (Table 1) we applied a random forest classifier to map habitat  
597 classes in the central Lena Delta and subsequently in the entire Lena Delta. Both maps represent  
598 the summer season of 2018 for which we could use a sufficient number of satellite images with low  
599 cloud cover.

Deleted: 4.2 Habitat class mapping<sup>¶</sup>

The identified habitat classes (Table 1) in the central Lena Delta were mapped with S-2 satellite data and a random forest classifier, achieving an overall class accuracy of 96.78% (Dataset 4). Additionally, the classification contains a water and a sand class, which were derived separately based on band masking thresholds. The central Lena Delta classification depicts both the different vegetation types, such as 'wet sedge', 'dry tundra' and 'dry shrub communities', but also the varying moisture regimes and surface water contributions, for example for the 'polygonal tundra complex' in the central delta. <sup>¶</sup>

Polygonal tundra is characterized by high spatial heterogeneity; at the meter-scale plant composition and diversity is defined by the polygonal microrelief and water level .

619 [The Lena Delta](#) habitat map shows the ice-rich first and third terraces mainly covered by i) the  
620 'polygonal tundra complex' due to impeded drainage on the terrace plateaus and by ii) drier tundra  
621 communities on well drained areas due to older degraded permafrost forms (detailed description in  
622 Morgenstern et al., 2008, 2011). On the second terrace, the classified 'dry dwarf shrub and herb  
623 communities' occur well separated from the moist habitat classes covering the floor of the alases.  
624 On the floodplains, the rich mosaic outlines a wide spectrum of very diverse classes, the dry versus  
625 moist and wet substrate habitats, in the active delta area.

626 [Polygonal tundra is characterized by high spatial heterogeneity; at the decimeter to meter-scale  
627 plant composition and diversity is defined by the polygonal microrelief and water level \(Whitaker and  
628 Woodwell, 1968; Forman and Godron, 1981; Zibulski et al., 2016; Nitzbon et al., 2020, Siewert et al.,  
629 2021\). Therefore, within a single S-2 pixel, dry polygonal rims, moist slopes, wet patches and  
630 surface water can all be present. The spatial resolution of S-2 cannot capture the meter-scale, but  
631 captures the heterogeneity between the different surface water contributions of the 'polygonal tundra  
632 complex' on the first and third terrace.](#) In the Lena Delta, the 'polygonal tundra complex with up to  
633 50% surface water' represents the dominant habitat class with 25% of the delta area (about 7 434  
634 km<sup>2</sup>). All other habitat classes represent 1-6% of the delta area with 'dwarf shrub-herb communities'  
635 and 'moist to wet sedge complex' reaching 5.4% and 5.9%, respectively (Figure 6). Based on the  
636 summer S-2 mosaic, the classes 'Water' and 'Sand' cover more than 40% of the delta. However,  
637 those two classes are extremely variable within and across years, depending on the river water level  
638 during image acquisition time. To provide information on this variability, we calculated how often  
639 each pixel in the delta (cloud free S-2 pixels from 2015 to 2022) was classified as sand (threshold  
640 approach). This led to an additional sand probability layer with values between 0-100%.

641 Despite extensive research within the area, only a few classification products are available for the  
642 Lena Delta. The new Lena Delta classification is a high-resolution (S-2, 10 m) map that focuses on  
643 the delta-specific habitat classes and emphasizes the high level of heterogeneity across the delta.  
644 We compared the Lena Delta habitat classification to existing classifications: the first published Lena  
645 Delta-wide land cover classification targeted towards tundra environments and the upscaling of  
646 methane emissions with 30 m resolution ([Schneider et al., 2009](#)), the global ESA Climate Change  
647 Initiative [CCI](#) land cover classification with 300 m resolution ([Defourny, 2019](#)), and a circum-arctic  
648 standardized ESA GlobPermafrost land cover map of the Lena Delta with 20 m resolution ([Bartsch  
649 et al., 2019](#)). We sampled the classification results with a regular point grid of more than 3 million  
650 points which have an equal distance of 100 m to one another to compare the classification results.  
651 Figures and tables with more information on class comparisons can be found in the supplements  
652 (Table 1, Figure S3, S4m, S5). Overall, the classifications of the Lena Delta overlap well for 'water'

Moved down [1]: Therefore, within a single S-2 pixel, dry polygonal rims, moist slopes, wet patches and surface water can all be present. The spatial resolution of S-2 cannot capture the meter-scale, but captures the heterogeneity between the different surface water contributions of the 'polygonal tundra complex' on the first and third terrace.

Deleted: Field expertise and expert knowledge were key to accomplish the classification and verify its high accuracy.¶  
The central Lena Delta classification was the basis for a delta-wide classification (Figure 5a, Dataset 5). We defined ESUs for the missing habitat class on the second terrace, produced an optimized standardized input dataset (S-2, Jun-Sept 2018), and applied the best performing classification algorithm (random forest classifier), to obtain a similarly high classification accuracy (98.6 % within the central Lena Delta), covering all three geomorphological terraces. ¶  
The

Moved (insertion) [1]

Deleted: 5

Deleted: Sentinel

Deleted: ,

Deleted: ,

Deleted: .

Deleted: XX

679 (water bodies (Defourny, 2019), shallow water (Schneider et al., 2009), water (different depths and  
680 sediment yields, Bartsch et al. 2019)) and 'sand' (bare areas (Defourny, 2019), mainly non-  
681 vegetated areas (Schneider et al., 2009), sand, seasonally inundated and disturbed (Bartsch et al.  
682 2019)) areas. Besides this, the mapped classes differ greatly from one another. For example, the  
683 dominant classes in the coarse ESA CCI land cover 2018 product (300 m) for the Lena Delta are  
684 'shrub or herbaceous cover', 'flooded', 'fresh / saline / brackish water', 'sparse vegetation (tree,  
685 shrub, herbaceous cover) (<15%)', and 'mosaic tree and shrub (>50%)', 'herbaceous cover (>50%)'.

686 These broad classes describe the major land cover in the Arctic delta but fail to depict the  
687 heterogeneity of habitats and plant communities not only because of its coarse spatial resolution but  
688 also because of the broad class descriptions. Furthermore, smaller areas are classified as 'tree  
689 cover', 'needleleaved', 'evergreen / deciduous', 'closed to open (>15%)' and 'mosaic tree and shrub  
690 (>50%) / herbaceous cover (<50%)' which is an inaccurate depiction of the delta.

691 This habitat map and the land cover classification from Schneider et al. (2009) resemble each other  
692 more closely, however, this habitat map shows more differentiation in the classes and spatial  
693 resolution, 10 m to 30 m, respectively. The only class description that is identical in both  
694 classifications, besides water and sand / mainly non-vegetated areas, is 'dry tussock tundra'.

695 However, there is only a small match between these classes in the point comparison and most 'dry  
696 tussock tundra' areas from the Schneider et al. (2009) classification fall into the PC\_50%, PC\_20%,  
697 'moist wet sedge complex' and 'dwarf shrub-herb communities'. The habitat map shows the mosaic  
698 of habitats on the floodplain with 'moist equisetum and shrubs on floodplain', 'dry low shrub  
699 community', 'moist to wet sedge' and 'wet sedge complex' which match with 'moist to dry dwarf  
700 shrub-dominated tundra' in the land cover classification of Schneider et al. (2009). Also, for the  
701 polygonal tundra complex, our habitat map shows more differentiation with three classes of up to  
702 50% 20% 10% surface water contribution versus two classes in Schneider et al. (2009) 'wet sedge  
703 and moss dominated tundra' and 'moist grass and moss dominated tundra' The areas covered by  
704 'PC\_50%' and 'PC\_20%' match with 'wet sedge- and moss-dominated tundra', and 'PC\_20%' and  
705 'PC\_10%' match with 'moist grass and moss-dominated tundra'. The overall aim of both maps is to  
706 differentiate between dry to wet land cover habitats as these describe the heterogeneity in the delta  
707 well and determine factors related to methane emissions (see Schneider et al. 2009) and the  
708 different habitat classes.

709 The land cover classification from ESA GlobPermafrost differentiates between 21 classes which are  
710 associated to eight broader groups, such as sparse vegetation, shrub tundra, forest, grassland,  
711 floodplain, disturbed, barren and water (Bartsch et al., 2019). With a spatial resolution of 20 m, the  
712 latter product is the closest to this habitat map. The major class 'wet ecotopes' of ESA

Deleted: ,

Deleted: ,

Deleted: (Fig. Sx)

Deleted: dwarsh

Deleted: .

Deleted: types/

Deleted: .

720 GlobPermafrost match with our 'PC\_50%:' on the first terrace and the 'moist to wet sedge complex'  
721 on the floodplains. On the floodplain however, other classes show less agreement. The ESA  
722 GlobPermafrost one class 'floodplain mostly fluvial' does not differentiate the floodplain classes  
723 further, in contrast to our habitat map differentiating between 'moist to wet sedge complex', 'wet  
724 sedge complex', 'moist equisetum and shrubs' and 'dry low shrub community' on floodplain.  
725 Whereas the ESA GlobPermafrost class 'disturbed' (defined as forest fire scars, seasonally  
726 inundation and landslide scars can be found in 'PC\_50%' predominantly, in 'sand', 'PC\_20%' and  
727 'sparsely vegetated areas' in our habitat map. This underlines the complex structure of match and  
728 mismatch between classifications.

Deleted: beweeen

Deleted: ,

729 The land cover map from Schneider et al. (2009) is based on two cloud-free Landsat images from  
730 June/July 2000 and 2001, the ESA CCI land cover 2018 map is based on summer images as well.  
731 Hence, the images used for this habitat classification were acquired at a similar time as for the ESA  
732 CCI product and we do not expect differences based on changes on the ground due to this temporal  
733 concurrence. In the almost 20-year difference between Schneider et al. (2009) and this habitat map  
734 we do expect changes in vegetation composition. Overall, it is challenging to obtain sufficient cloud-  
735 free images during the summer months to fully cover the entire Lena Delta for a classification project  
736 and to depict a specific phenological state. Therefore, we created a Sentinel-2 composite mosaic  
737 based on the maximum NDVI value per pixel from June to September. With this we ensure to have  
738 the peak vegetation and phenology season represented as input for the habitat classification as  
739 much as possible and increase comparability to other classification studies despite a temporal  
740 mismatch.

741 The habitat map gives an accurate and detailed description of the Arctic Lena Delta that  
742 incorporates extensive field data and expert knowledge. The habitat map is superior to the ESA CCI  
743 land cover map (2018) in both spatial resolution and class description as it depicts the  
744 heterogeneous habitat distribution. The 20m ESA GlobPermafrost classification matches the  
745 resolution of the habitat map closely but due to its wider geographical application with circum-Arctic  
746 standardized classes it does not optimally represent Lena Delta-specific habitats, such as the widely  
747 distributed polygonal tundra complex. Furthermore, the habitat map is an update to Schneider et al.  
748 (2009), which was based on three Landsat images from 2000 and 2001 and shows further  
749 differentiation of habitats, specifically representing the floodplain mosaics of this Arctic delta.

Deleted: a highly

#### 750 **4.3 Habitat linked disturbance regimes**

Deleted: 2

751 Parts of the Lena Delta are characterised by disturbances due to annual floodings or rapid  
752 permafrost thaw processes leading to specific habitat classes. We provide habitat linked disturbance

Deleted: an upscaling product of

758 regimes (describing the type and intensity of disturbances) across the delta. Our product (Dataset 6,  
759 Figure 6a) shows that the largest part of the vegetated delta (excluding 12 439 km<sup>2</sup> of 'sand' and  
760 'water' classes) is impacted by low disturbance, resulting in mature-state plant communities on the  
761 terrace plateaus (Figure 6b, 72%, 12 806 km<sup>2</sup>). Specifically, the second terrace in the northwest of  
762 the delta, with low ice content, is least impacted by rapid thaw processes and not part of the active  
763 delta. In contrast, the habitats in the active delta are all linked to high disturbance (27%, 4 875 km<sup>2</sup>).  
764 The 'moist to wet sedge complex' (10% of the vegetated Lena Delta) is the largest class considered  
765 to be formed by high disturbance. This class is found in larger patch sizes on the riverine floodplains,  
766 smaller patches on the floor of thermo-erosional valleys. Overall, 27.5% of the vegetated area of the  
767 Lena Delta experiences some level of high disturbance from either regular spring floods or from  
768 rapid thaw processes.

769 Species richness, relative abundance and biomass characteristics are important habitat features that  
770 are influenced by landscape characteristics such as topography, water fluxes, soil types and  
771 disturbance regimes (Forman and Godron, 1981; Naiman et al., 1986; Pickett et al., 1989;  
772 Montgomery, 1999). Greig-Smith (1964), Woodwell and Whittaker (1968), and Forman and Godron  
773 (1981) described fragmentation of land surfaces due to disturbance (defined by type and intensities)  
774 and topography. In the Lena Delta, the terrace-related topography and active floodplain areas are  
775 major determinants of plant communities and habitat classes and are thus well reflected in the Lena  
776 Delta habitat map.

777 The high disturbance regime on floodplains results in 'shifting habitats' (Stanford et al., 2005; Driscoll  
778 and Hauer, 2019). The annual spring floods and rapid thaw processes result in areas of high  
779 disturbances, habitats of mid to advanced plant successional stages showing high vascular plant  
780 above ground biomass (Figure 6c) due to the higher nutrient availability, a deeper active layer and  
781 more moisture (e.g., Myers-Smith et al., 2020). Within the low disturbance habitat classes, a thick  
782 moss layer as well as a low vascular plant coverage characterise the tundra community  
783 assemblages representing mature state plant communities. Because high disturbance patches are  
784 characterized by high vascular biomass, they can be well classified specifically in the NDVI, but also  
785 NIR and red edge bands of optical medium resolution sensors such as S-2. Within the vegetation  
786 plots (Dataset 1), we did not find clear differences in species richness and in the Shannon diversity  
787 index between the disturbed and the undisturbed classes (Figure 6d). Since most disturbed habitat  
788 classes such as the 'moist to wet sedge', the 'wet sedge' as well as homogeneous patches of high  
789 shrubs (as part of the habitat class 'dry grass to wet sedge complex'), were not sampled in the field  
790 due to too challenging conditions, however they are clearly representing habitats with low species  
791 richness. In the extreme case disturbance can lead to barren and sparsely vegetated surfaces.

Deleted: 5a

Deleted: 5b

Deleted: 5c

Deleted: S2

Deleted: 5d

#### 4.4 Classification accuracy and representativeness

The field data was acquired during a field trip in July-August 2018, primarily focusing on 30 m x 30 m homogeneous vegetation and land cover plots. Additionally, we relied on Sentinel-2 images for the different classifications that were also acquired in summer 2018, covering the same period as the field trip, and have a spatial resolution of 20 m. The temporal overlap of the field work and the satellite image acquisitions ensures consistency across the different datasets and represents a close relationship between datasets and products obtained in the field (dataset 1, 2 and 3) and the results derived from the satellite images that use the field data as input. As Sentinel-2 images have a small geolocation error, we could link our field plot locations directly with the satellite images. Furthermore, the sampling and measurement design of the plots with 30 m x 30 m ensured a reliable link to the satellite data with similar spatial resolution, as we followed the recommendations on ESU. The RGBNIR Sentinel-2 bands have a spatial resolution of 10 m and the red edge (NIR) and SWIR bands a spatial resolution of 20 m, and even if we downsampled the bands to 10 m the spectral information is sustained. More information on datasets and their spatial and temporal resolutions are provided in supplementary Table S3.

The presented datasets are limited by the regional in-situ observations and expert knowledge collected mainly in the central Lena Delta. The remoteness of the area and extremely difficult logistics to conduct research in the second terrace and the outer rims of the delta are major reasons for these limitations. However, the delta is relatively homogeneous in habitat classes that develop based on underlying geomorphology and the disturbance regime (annual flooding and permafrost thaw processes). Only one major habitat class is absent from the well studied central Lena Delta and only occurs across the second terrace. Thus, even though detailed knowledge and in-situ observations are derived from a relatively small subset of the Delta, we are confident that our mapping results from the entire region are valuable and accurate. Also due to the inaccessibility of large areas of the delta, quantitative accuracy assessments of the classifier and the final mapping product are lacking. We had to rely on qualitative evaluation procedures by experts. Analysis of similarity of habitat classes and S-2 spectral reflectance as well as NDVI values provide additional quantitative and qualitative assessments on the extent to which the different classes are identifiable and separated between classes.

In-situ observations (Datasets 1-3) as well as mapping products (Datasets 4-6) represent conditions and vegetation composition of 2018. The timing of the summer 2018 expedition coincided with a relatively high number of cloud free S-2 images necessary for a high quality habitat classification. Overall, the described datasets are of appropriate quality to serve as a basis for additional studies and most importantly as a baseline to identify changes in the future.

831 **5 Conclusions**

832 The described datasets provide coherent and complementary information of the major habitat  
833 classes in the Lena Delta in Arctic Siberia, the largest delta in the Arctic. Based on extensive  
834 knowledge collected during fieldwork that included habitat-related measurements of plant  
835 composition, biomass, and hyperspectral field measurements we provide a validated and high-  
836 resolution habitat classification map of the delta. In addition, we linked ecologically important  
837 characteristics of disturbances in the delta to habitat classes, providing a baseline for future studies  
838 of Arctic change as well as a foundation for potential upscaling of related processes such as  
839 biodiversity, ecosystem functions, and biochemical dynamics such as greenhouse gas emissions.  
840 With this update of previous land cover and habitat-related mapping products of the Lena Delta we  
841 strive to facilitate and promote future investigations leading to a better understanding of this highly  
842 sensitive arctic delta system.

843 **Acknowledgements**

844 Field work in the Lena River Delta was conducted in the frame of the Russian-German LENA  
845 Expeditions based at Research Station Samoylov Island. We thank all colleagues and station staff  
846 involved in the organization and logistics for their great support.

847 **Code/Data availability**

848 [Dataset 1: Shevtsova et al., 2021a, https://doi.pangaea.de/10.1594/PANGAEA.935875](https://doi.pangaea.de/10.1594/PANGAEA.935875), Foliage  
849 projective cover of 26 vegetation sites in the central Lena Delta from 2018, is published as Foliage  
850 projective cover for all major taxa estimated as percent, as tab-delimited text files.

851 [Dataset 2: Shevtsova et al., 2021b, https://doi.pangaea.de/10.1594/PANGAEA.935923](https://doi.pangaea.de/10.1594/PANGAEA.935923), Total above-  
852 ground biomass of 25 vegetation sites in the central Lena Delta from 2018, is published as biomass  
853 aboveground dry mass per major taxa, as well as for 'moss and lichen', 'litter' and the remaining minor  
854 taxa (called 'other plants') and the total biomass in the units [g/m2], as tab-delimited text.

855 [Dataset 3: Runge et al., 2022, https://doi.pangaea.de/10.1594/PANGAEA.945982](https://doi.pangaea.de/10.1594/PANGAEA.945982), Hyperspectral field  
856 spectrometry of Arctic vegetation units in the central Lena Delta, is published as an overview of the  
857 plot details and field spectrometer reflectance spectra in the unit [%] of 28 vegetation plots, as tab-  
858 delimited text files.

Deleted: Dataset 1: ¶  
Dataset 2: ¶  
Dataset 3: ¶  
Dataset 4: ¶  
Dataset 5: ¶  
Dataset 6:

865 [Dataset 4: Landgraf et al., 2022 a.b.c. The Sentinel-2-derived central Lena Delta land cover \(habitat\)](#)  
866 [classification consists of the following three data publications: i\) Landgraf et al. 2022a,](#)  
867 <https://doi.pangaea.de/10.1594/PANGAEA.945056>: a raster file with assigned land cover classes and an  
868 [ESRI polygon shape file containing the 10 training classes representing the different vegetation](#)  
869 [compositions, as geotiff file. Both datasets are based on 2018 satellite images and informed by the in-](#)  
870 [situ vegetation plots and expert knowledge. Datasets are in Universe Transverse Mercator \(UTM\) Zone](#)  
871 [52 North projection. ii\) Landgraf et al. 2022b, https://doi.pangaea.de/10.1594/PANGAEA.945054. This](#)  
872 [data set includes training elements representing different vegetation composition in the form of](#)  
873 [Elementary Sampling Units ESUs: 69 pseudo ESUs set with expert knowledge from the field and from](#)  
874 [Lena Delta expedition field reports. iii\) Landgraf et al. 2022c,](#)  
875 <https://doi.pangaea.de/10.1594/PANGAEA.945055>. This data set includes training elements representing  
876 [different vegetation composition in the form of Elementary Sampling Units ESUs: 23 true ESUs](#)  
877 [representing the LD18 vegetation plots.](#)

878 [Dataset 5: Lisovski et al., 2022, https://doi.pangaea.de/10.1594/PANGAEA.946407. The Lena Delta](#)  
879 [Habitat Map \(2018, Sentinel-2\) contains i\) the Lena Delta habitat map \(13 classes\), ii\) the sand probability](#)  
880 [map, both as geotiff files in WGS84 geographic projection, iii\) the habitat class description as comma](#)  
881 [delimited csv table, and iv\) the training dataset \(n = 4 278 classified pixels\) in geographic decimal](#)  
882 [coordinates comma delimited csv table. The data collection also contains the Lena Delta Region of](#)  
883 [Interest \(ROI\) ESRI shapefile outlining the Lena Delta including a coastal water buffer.](#)

884 [Dataset 6: Heim and Lisovski, 2023, https://doi.org/10.5281/zenodo.7575691. The Lena Delta habitat](#)  
885 [disturbance regime map is published in the form of two geotiff files \(tiles\) in WGS84 geographic](#)  
886 [projection.](#)

887 [Code developed in Google Earth Engine to derive habitat classes based in the central Lena Delta](#)  
888 [classification, as well as R code for figures can be accessed from the following repository: Lisovski,](#)  
889 [S. \(2024\). Code for 'A new habitat map of the Lena Delta in Arctic Siberia based on field and remote](#)  
890 [sensing datasets'. V0.1. Zenodo. 10.5281/zenodo.11197641.](#)

## 891 Competing interests

892 Birgit Heim is a member of the editorial board of ESSD. Otherwise, we declare no competing interests.

893 **Funding**

894 SL acknowledges funding from the Geo.X Network for Geosciences in Berlin and Brandenburg. This  
895 study was supported by BMBF KoPf (Grant Number 03F0764B), KoPf Synthesis (Grant Number  
896 03F0834B), and AWI base funds. AR was partially funded by ESA GlobPermafrost and an ESA CCI  
897 postdoctoral fellowship. BH acknowledges HGF REKLIM.

898 **Authors contribution**

899 SL: Conceptual framework, habitat classification, data analysis, writing

900 AR: Conceptual framework, field work, spectral field data collection, habitat classification, spectral  
901 data processing, data analysis, writing

902 IS: Field work, [biomass and projective cover measurement in vegetation plots](#), habitat classification

Deleted: data collection, concept of

Deleted: sampling

903 RRO: Habitat classification

904 NL: [habitat](#) classification, spectral data processing

Deleted: Habitat

905 MF: Field work, spectral field data collection

906 [NiL](#): habitat [class](#) definition, [field work](#)

Deleted: NL

907 AM: Project management, writing

908 [CS](#): [Spectral data](#) processing

Deleted: AB: Protocol and code for field spectrometry

909 [AB](#): [Spectral data](#) processing

Deleted: CS: Field spectrometry

910 [UH](#): [Conceptual framework](#), [project management](#)

911 GG: [Conceptual framework](#), [project management](#), habitat classification, writing

Deleted: Project

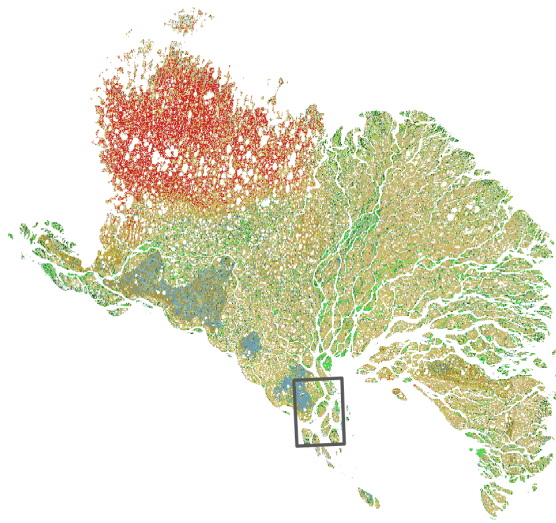
912 [BH](#): Conceptual framework, [field work](#), habitat classification, [project management](#), [writing](#)

Deleted: UH: Project management, concept of  
vegetation & biomass sampling, co-supervision of field  
data analyses

Deleted: field work, data collection,

913

925 Appendix



926  
927 Figure A1: Location of the central Lena Delta (Dataset 4) in the Lena Delta (Dataset 5.6). WGS 84 projection.

928  
929

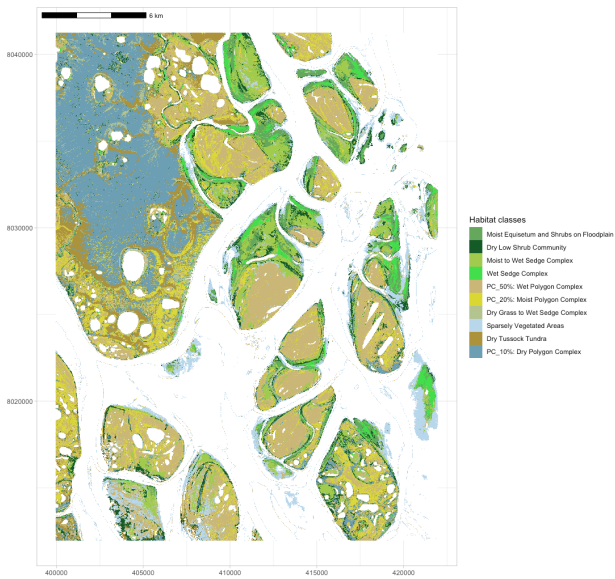
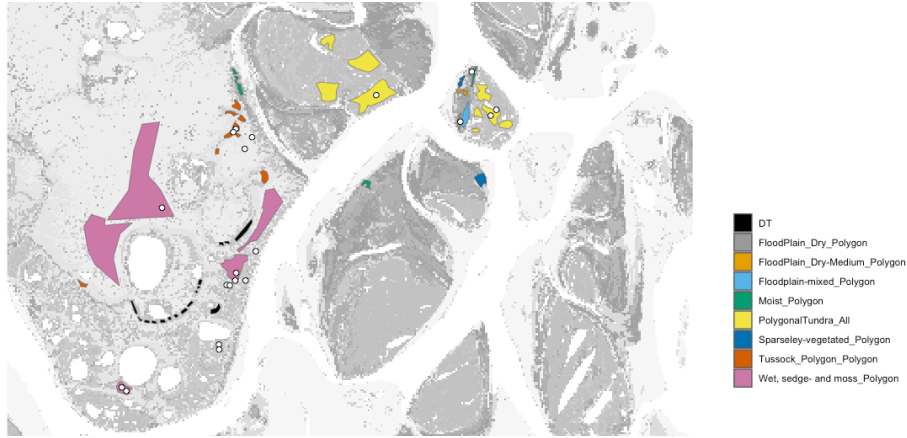
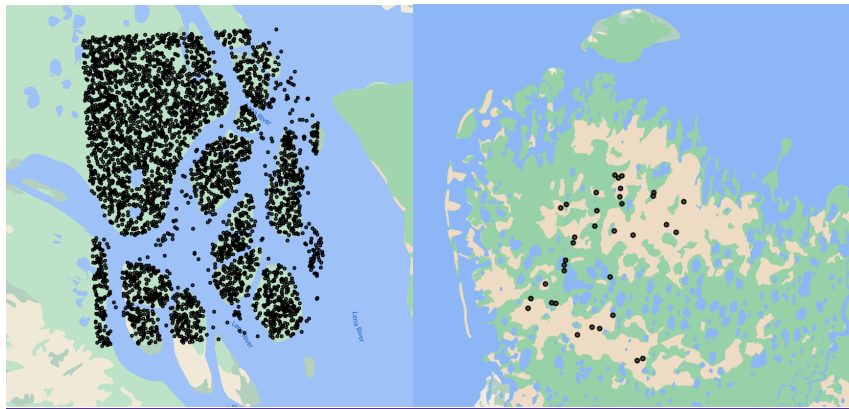


Figure A2: Supervised habitat classification of the central Lena Delta based on a cloud-free S-2 August 2018 acquisition (Dataset 4). Numbers in legend correspond to the labels in published Dataset 4 (Landgraf et al. 2022). Universe Transverse Mercator Z52 on WGS 84 projection.



951  
 952 **Figure A3:** Subset of the central Lena Delta with 30 x 30 m ESUs (white points, dataset 1) and polygons defined by  
 953 expert knowledge (published with dataset 4). Together the ESUs and polygons served areas to sample 8 626 training  
 954 pixels for the central Lena Delta landcover/habitat classification (dataset 4, Landgraf et al. 2022a).  
 955  
 956



957  
 958 **Figure A4:** Training pixels for the Lena Delta habitat classification (dataset 5). (Left) 7,500 random pixels samples  
 959 across the habitat classes from the central Lena Delta landcover/habitat map (dataset 4). (Right) 35 pixels selected  
 960 by expert knowledge for the 'dwarf shrub - herb communities' that are missing in the central Lena Delta.  
 961

## 962 References

963 [AMAP: AMAP Arctic Climate Change Update 2021: Key Trends and Impacts. Arctic Monitoring](#)  
964 [and Assessment Programme \(AMAP\), Tromsø, Norway, viii+148pp, 2021.](#)

965 [Bartlett, K. B., Crill, P. M., Sass, R. L., Harriss, R. C., and Dise, N. B.: Methane Emissions from](#)  
966 [Tundra Environments in the Yukon-Kuskokwim Delta, Alaska, Journal of Geophysical](#)  
967 [Research-Atmospheres, 97, 16645-16660, doi: 10.1029/91jd00610, 1992.](#)

968 [Bartsch, A., Hofler, A., Kroisleitner, C., and Trofaier, A. M.: Land Cover Mapping in Northern](#)  
969 [High Latitude Permafrost Regions with Satellite Data: Achievements and Remaining](#)  
970 [Challenges, Remote Sensing, 8, 979, doi: 10.3390/rs8120979, 2016.](#)

971 [Bartsch, A., Widhalm, B., Pointner, G., Ermokhina, K., Leibman, M., and Heim, B.: Landcover](#)  
972 [derived from Sentinel-1 and Sentinel-2 satellite data \(2015-2018\) for subarctic and arctic](#)  
973 [environments \[dataset\], <https://doi.org/10.1594/PANGAEA.897916>, 2019.](#)

974 [Bartsch, A., Widhalm, B., Leibman, M., Ermokhina, K., Kumpula, T., Skarin, A., Wilcox, E. J.,](#)  
975 [Jones, B. M., Frost, G. V., Hofler, A., and Pointner, G.: Feasibility of tundra vegetation height](#)  
976 [retrieval from Sentinel-1 and Sentinel-2 data, Remote Sensing of Environment, 237, 111515,](#)  
977 [doi: 10.1016/j.rse.2019.111515, 2020.](#)

978 [Beamish, A., Reynolds, M. K., Epstein, H., Frost, G. V., Macander, M. J., Bergstedt, H., Bartsch,](#)  
979 [A., Kruse, S., Miles, V., Tanis, C. M., Heim, B., Fuchs, M., Chabrillat, S., Shevtsova, I.,](#)  
980 [Verdonen, M., and Wagner, J.: Recent trends and remaining challenges for optical remote](#)  
981 [sensing of Arctic tundra vegetation: A review and outlook, Remote Sensing of Environment,](#)  
982 [246, ARTN 111872, doi: 10.1016/j.rse.2020.111872, 2020.](#)

983 [Beamish, A. L., Coops, N., Chabrillat, S., and Heim, B.: A Phenological Approach to Spectral](#)  
984 [Differentiation of Low-Arctic Tundra Vegetation Communities, North Slope, Alaska, Remote](#)  
985 [Sensing, 9, 1200, doi: 10.3390/rs9111200, 2017.](#)

986 [Beamish, A. L., Coops, N. C., Hermosilla, T., Chabrillat, S., and Heim, B.: Monitoring pigment-](#)  
987 [driven vegetation changes in a low-Arctic tundra ecosystem using digital cameras, Ecosphere,](#)  
988 [9, e02123, doi: 10.1002/ecs2.2123, 2018.](#)

989 [Berner, L. T., Massey, R., Jantz, P., Forbes, B. C., Macias-Fauria, M., Myers-Smith, I.,](#)  
990 [Kumpula, T., Gauthier, G., Andreu-Hayles, L., Gaglioti, B. V., Burns, P., Zetterberg, P., D'Arrigo,](#)  
991 [R., and Goetz, S. J.: Summer warming explains widespread but not uniform greening in the](#)  
992 [Arctic tundra biome, Nature Communications, 11, 4621, doi: 10.1038/s41467-020-18479-5,](#)  
993 [2020.](#)

994 [Biskaborn, B. K., Smith, S. L., Noetzli, J., Matthes, H., Vieira, G., Streletskiy, D. A., Schoeneich,](#)  
995 [P., Romanovsky, V. E., Lewkowicz, A. G., Abramov, A., Allard, M., Boike, J., Cable, W. L.,](#)  
996 [Christiansen, H. H., Delaloye, R., Diekmann, B., Drozdov, D., Etzelmuller, B., Grosse, G.,](#)  
997 [Guglielmin, M., Ingeman-Nielsen, T., Isaksen, K., Ishikawa, M., Johannsson, M., Johannsson, H.,](#)  
998 [Joo, A., Kaverin, D., Kholodov, A., Konstantinov, P., Kroger, T., Lambiel, C., Lanckman, J. P.,](#)  
999 [Luo, D. L., Malkova, G., Meiklejohn, I., Moskalenko, N., Oliva, M., Phillips, M., Ramos, M.,](#)  
1000 [Sannel, A. B. K., Sergeev, D., Seybold, C., Skryabin, P., Vasiliev, A., Wu, Q. B., Yoshikawa, K.,](#)  
1001 [Zheleznyak, M., and Lantuit, H.: Permafrost is warming at a global scale. Nature](#)  
1002 [Communications, 10, 264, doi: 10.1038/s41467-018-08240-4, 2019.](#)

1003 [Boike, J., Wille, C., and Abnizova, A.: Climatology and summer energy and water balance of](#)  
1004 [polygonal tundra in the Lena River Delta, Siberia, Journal of Geophysical Research-](#)  
1005 [Biogeosciences, 113, G03025, doi: 10.1029/2007jg000540, 2008.](#)

1006 [Boike, J., Nitzbon, J., Anders, K., Grigoriev, M., Bolshiyarov, D., Langer, M., Lange, S.,](#)  
1007 [Bornemann, N., Morgenstern, A., Schreiber, P., Wille, C., Chadburn, S., Gouttevin, I., Burke, E.,](#)  
1008 [and Kutzbach, L.: A 16-year record \(2002-2017\) of permafrost, active-layer, and meteorological](#)  
1009 [conditions at the Samoylov Island Arctic permafrost research site, Lena River delta, northern](#)  
1010 [Siberia: an opportunity to validate remote-sensing data and land surface, snow, and permafrost](#)  
1011 [models, Earth System Science Data, 11, 261-299, doi: 10.5194/essd-11-261-2019, 2019.](#)

1012 [Box, J. E., Colgan, W. T., Christensen, T. R., Schmidt, N. M., Lund, M., Parmentier, F. J. W.,](#)  
1013 [Brown, R., Bhatt, U. S., Euskirchen, E. S., Romanovsky, V. E., Walsh, J. E., Overland, J. E.,](#)  
1014 [Wang, M. Y., Corell, R. W., Meier, W. N., Wouters, B., Mernild, S., Mard, J., Pawlak, J., and](#)  
1015 [Olsen, M. S.: Key indicators of Arctic climate change: 1971-2017, Environmental Research](#)  
1016 [Letters, 14, 045010, doi: 10.1088/1748-9326/aafc1b, 2019.](#)

1017 [Buchhorn, M., Walker, D. A., Heim, B., Reynolds, M. K., Epstein, H. E., and Schwieder, M.:](#)  
1018 [Ground-Based Hyperspectral Characterization of Alaska Tundra Vegetation along](#)  
1019 [Environmental Gradients, Remote Sensing, 5, 3971-4005, doi: 10.3390/rs5083971, 2013.](#)

1020 [Driscoll, K. P. and Hauer, F. R.: Seasonal flooding affects habitat and landscape dynamics of a](#)  
1021 [gravel-bed river floodplain. \*Freshwater Science\*, 38, 510-526, doi: 10.1086/704826, 2019.](#)

1022 [Drusch, M., Del Bello, U., Carlier, S., Colin, O., Fernandez, V., Gascon, F., Hoersch, B., Isola,](#)  
1023 [C., Laberinti, P., Martimort, P., Meygret, A., Spoto, F., Sy, O., Marchese, F., Bargellini, P.,](#)  
1024 [Sentinel-2: ESA's optical high-resolution mission for GMES operational services. \*Rem. Sens.\*](#)  
1025 [Environ., 120, 25–36, doi: 10.1016/j.rse.2011.11.026 , 2012.](#)

1026 [Duncanson, L., Armston, J., Disney, M., Avitabile, V., Barbier, N., Calders, K., Carter, S.,](#)  
1027 [Chave, J., Herold, M., MacBean, N., McRoberts, R., Minor, D., Paul, K., Réjou-Méchain, M.,](#)  
1028 [Roxburgh, S., Williams, M., Albinet, C., Baker, T., Bartholomeus, H., Bastin, J. F., Coomes, D.,](#)  
1029 [Crowther, T., Davies, S., de Bruin, S., De Kauwe, M., Domke, G., Dubayah, R., Falkowski, M.,](#)  
1030 [Fatoyinbo, L., Goetz, S., Jantz, P., Jonckheere, I., Jucker, T., Kay, H., Kellner, J., Labriere, N.,](#)  
1031 [Lucas, R., Mitchard, E., Morsdorf, F., Næsset, E., Park, T., Phillips, O. L., Ploton, P., Puliti, S.,](#)  
1032 [Quegan, S., Saatchi, S., Schaaf, C., Schepaschenko, D., Scipal, K., Stovall, A., Thiel, C.,](#)  
1033 [Wulder, M. A., Camacho, F., Nickeson, J., Román, M., and Margolis, H.: Aboveground Woody](#)  
1034 [Biomass Product Validation Good Practices Protocol. Version 1.0, Land Product Validation](#)  
1035 [Subgroup \(WGCV/CEOS\), doi:10.5067/doc/ceoswgcv/lpv/agb.001, 2021.](#)

1036 [Endsley, K. A., Kimball, J. S., and Reichle, R. H.: Soil Respiration Phenology Improves Modeled](#)  
1037 [Phase of Terrestrial net Ecosystem Exchange in Northern Hemisphere. \*Journal of Advances in\*](#)  
1038 [Modeling Earth Systems, 14, e2021MS002804, doi: 10.1029/2021MS002804, 2022.](#)

1039 [ESA, 2015. Sentinel-2 User Handbook. ESA Standard Document.](#)

1040 [ESA Land Cover CCI project team; Defourny, P. \(2019\): ESA Land Cover Climate Change](#)  
1041 [Initiative \(Land\\_Cover\\_cci\): Global Land Cover Maps, Version 2.0.7. Centre for](#)  
1042 [Environmental Data Analysis, \*downloaded 2022\*, \[dataset\]](#)  
1043 <https://catalogue.ceda.ac.uk/uuid/b382ebe6679d44b8b0e68ea4ef4b701c>

1044 [Fedorova, I., Chetverova, A., Bolshiyarov, D., Makarov, A., Boike, J., Heim, B., Morgenstern,](#)  
1045 [A., Overduin, P. P., Wegner, C., Kashina, V., Eulenburg, A., Dobrotina, E., and Sidorina, I.:](#)  
1046 [Lena Delta hydrology and geochemistry: long-term hydrological data and recent field](#)  
1047 [observations. \*Biogeosciences\*, 12, 345-363, doi: 10.5194/bg-12-345-2015, 2015.](#)

1048 [Forman, R. T. T. and Godron, M.: Patches and Structural Components for a Landscape](#)  
1049 [Ecology, Bioscience, 31, 733-740, doi 10.2307/1308780, 1981.](#)

1050 [Frost, G. V., Loehman, R. A., Saperstein, L. B., Macander, M. J., Nelson, P. R., Paradis, D. P.,](#)  
1051 [and Natali, S. M.: Multi-decadal patterns of vegetation succession after tundra fire on the](#)  
1052 [Yukon-Kuskokwim Delta, Alaska, Environmental Research Letters, 15, 025003, doi:](#)  
1053 [10.1088/1748-9326/ab5f49, 2020.](#)

1054 [Gilg, O., Sané, R., Solovieva, D. V., Pozdnyakov, V. I., Sabard, B., Tsanos, D., Zöckler, C.,](#)  
1055 [Lappo, E. G., Syroechkovski, J. E. E., and Eichhorn, G.: Birds and Mammals of the Lena Delta](#)  
1056 [Nature Reserve, Siberia, ARCTIC, 53, 118-133, doi: 10.14430/arctic842, 2000.](#)

1057 [Greig-Smith, P.: Quantitative plant ecology, Butterworths 1964.](#)

1058 [Grigoriev, M. N.: Crio Morphogenesis in the Lena Delta, Permafrost Institute Press, Yakutsk](#)  
1059 [1993.](#)

1060 [Heim, B. and Lisovski, S.: Lena Delta habitat disturbance regimes \(0.0\) \[dataset\], Zenodo,](#)  
1061 [https://doi.org/10.5281/zenodo.7575691, 2023.](#)

1062 [Holl, D., Wille, C., Sachs, T., Schreiber, P., Runkle, B. R. K., Beckebanze, L., Langer, M., Boike,](#)  
1063 [J., Pfeiffer, E. M., Fedorova, I., Bolshianov, D. Y., Grigoriev, M. N., and Kutzbach, L.: A long-](#)  
1064 [term \(2002 to 2017\) record of closed-path and open-path eddy covariance CO2 net ecosystem](#)  
1065 [exchange fluxes from the Siberian Arctic, Earth System Science Data, 11, 221-240, doi:](#)  
1066 [10.5194/essd-11-221-2019, 2019.](#)

1067 [Hu, F. S., Higuera, P. E., Duffy, P., Chipman, M. L., Rocha, A. V., Young, A. M., Kelly, R., and](#)  
1068 [Dietze, M. C.: Arctic tundra fires: natural variability and responses to climate change, Frontiers](#)  
1069 [in Ecology and the Environment, 13, 369-377, doi: 10.1890/150063, 2015.](#)

1070 [Hubberten, H.-W., Wagner, D., Pfeiffer, E.-M., Boike, J., and Gukov, A. Y.: The Russian-](#)  
1071 [German research station samoylov, Lena delta -A key site for polar research in the Siberian](#)  
1072 [arctic, Polarforschung, 2006.](#)

1073 [Jorgenson, M. T.: Hierarchical organisation of ecosystems at multiple spatial scales on the](#)  
1074 [Yukon-Kuskokwim Delta, Alaska, USA, Arctic Antarctic and Alpine Research, 32, 221-239, doi](#)  
1075 [10.2307/1552521, 2000.](#)

1076 [Juhls, B., Antonova, S., Angelopoulos, M., Bobrov, N., Grigoriev, M., Langer, M., Maksimov, G.,](#)  
1077 [Miesner, F., and Overduin, P. P.: Serpentine \(Floating\) Ice Channels and their Interaction with](#)  
1078 [Riverbed Permafrost in the Lena River Delta, Russia, \*Frontiers in Earth Science\*, 9, 689941, doi:](#)  
1079 [10.3389/feart.2021.689941, 2021.](#)

1080 [Kienast, F. and Tsherkasova, J.: Comparative botanical recent-studies in the Lena River Delta](#)  
1081 [\[Field Report\], Alfred Wegener Institute, Germany, 2001.](#)

1082 [Landgraf, N., Shevtsova, I., Pflug, B., and Heim, B. : Sentinel-2 derived central Lena Delta land](#)  
1083 [cover classification, PANGAEA \[dataset\], <https://doi.pangaea.de/10.1594/PANGAEA.945057>,](#)  
1084 [2022a.](#)

1085 [Landgraf, N., Shevtsova, I., Pflug, B., and Heim, B.: Raster file with assigned land cover classes](#)  
1086 [and ESRI polygon shape file training classes representing different vegetation composition,](#)  
1087 [PANGAEA \[dataset\], <https://doi.pangaea.de/10.1594/PANGAEA.945056>, 2022b.](#)

1088 [Landgraf, N., Shevtsova, I., Pflug, B., and Heim, B.: 23 true Elementary Sampling Units \(ESUs\)](#)  
1089 [set in the Lena Delta representing the LD18 vegetation plots, PANGAEA \[dataset\],](#)  
1090 [https://doi.pangaea.de/10.1594/PANGAEA.945055, 2022c.](#)

1091 [Landgraf, N., Shevtsova, I., Pflug, B., and Heim, B.: 69 pseudo Elementary Sampling Units](#)  
1092 [\(ESUs\) set in the Lena Delta derived with expert knowledge, PANGAEA \[dataset\],](#)  
1093 [https://doi.pangaea.de/10.1594/PANGAEA.945054, 2022d.](#)

1094 [Lantz, T. C., Kokelj, S. V., and Fraser, R. H.: Ecological recovery in an Arctic delta following](#)  
1095 [widespread saline incursion, \*Ecological Applications\*, 25, 172-185, doi: 10.1890/14-0239.1,](#)  
1096 [2015.](#)

1097 [Lisovski, S., Runge, A., Okoth, R. R., Shevtsova, I., and Heim, B.: Lena Delta Land Cover](#)  
1098 [Classification \(2018, Sentinel-2\), PANGAEA \[dataset\], doi: 10.1594/PANGAEA.946407, 2022.](#)

1099 [Lorang, M. S. and Hauer, F. R.: Fluvial geomorphic processes, in: \*Methods in stream ecology\*,](#)  
1100 [edited by: Hauer, F. R., and Lamberti, G. A., Academic Press/Elsevier, San Diego, 145–168,](#)  
1101 [2006.](#)

1102 [Macander, M. J., Nelson, P. R., Nawrocki, T. W., Frost, G. V., Orndahl, K. M., Palm, E. C.,](#)  
1103 [Wells, A. F., and Goetz, S. J.: Time-series maps reveal widespread change in plant functional](#)

1104 [type cover across Arctic and boreal Alaska and Yukon, Environmental Research Letters, 17,](#)  
1105 [ARTN 054042, doi: 10.1088/1748-9326/ac6965, 2022.](#)

1106 [Mauclet, E., Agnan, Y., Hirst, C., Monhonval, A., Pereira, B., Vandeuren, A., Villani, M.,](#)  
1107 [Ledman, J., Taylor, M., Jasinski, B. L., Schuur, E. A. G., and Opfergelt, S.: Changing sub-Arctic](#)  
1108 [tundra vegetation upon permafrost degradation: impact on foliar mineral element cycling,](#)  
1109 [Biogeosciences, 19, 2333-2351, doi: 10.5194/bg-19-2333-2022, 2022.](#)

1110 [Mekonnen, Z. A., Riley, W. J., Berner, L. T., Bouskill, N. J., Torn, M. S., Iwahana, G., Breen, A.](#)  
1111 [L., Myers-Smith, I. H., Criado, M. G., Liu, Y. L., Euskirchen, E. S., Goetz, S. J., Mack, M. C., and](#)  
1112 [Grant, R. F.: Arctic tundra shrubification: a review of mechanisms and impacts on ecosystem](#)  
1113 [carbon balance, Environmental Research Letters, 16, 053001, doi: 0.1088/1748-9326/abf28b,](#)  
1114 [2021.](#)

1115 [Montgomery, D. R.: Process domains and the river continuum, Journal of the American Water](#)  
1116 [Resources Association, 35, 397-410, doi: 10.1111/j.1752-1688.1999.tb03598.x, 1999.](#)

1117 [Morgenstern, A., Grosse, G., and Schirrmeyer, L.: Genetic, morphological, and statistical](#)  
1118 [characterization of lakes in the permafrost-dominated Lena Delta, Ninth International](#)  
1119 [Conference on Permafrost, 2008.](#)

1120 [Morgenstern, A., Grosse, G., Gunther, F., Fedorova, I., and Schirrmeyer, L.: Spatial analyses](#)  
1121 [of thermokarst lakes and basins in Yedoma landscapes of the Lena Delta, Cryosphere, 5, 849-](#)  
1122 [867, doi:10.5194/tc-5-849-2011, 2011.](#)

1123 [Morgenstern, A., Overduin, P. P., Gunther, F., Stettner, S., Ramage, J., Schirrmeyer, L.,](#)  
1124 [Grigoriev, M. N., and Grosse, G.: Thermo-erosional valleys in Siberian ice-rich permafrost,](#)  
1125 [Permafrost and Periglacial Processes, 32, 59-75, doi: 10.1002/ppp.2087, 2021.](#)

1126 [Morgenstern, A., Ulrich, M., Gunther, F., Roessler, S., Fedorova, I. V., Rudaya, N. A., Wetterich,](#)  
1127 [S., Boike, J., and Schirrmeyer, L.: Evolution of thermokarst in East Siberian ice-rich](#)  
1128 [permafrost: A case study, Geomorphology, 201, 363-379, doi:](#)  
1129 [10.1016/j.geomorph.2013.07.011, 2013.](#)

1130 [Mueller-Bombois, D. and Ellenberg, H.: Aims and methods of vegetation ecology, John Wiley &](#)  
1131 [Sons, New York, USA1974.](#)

1132 [Myers-Smith, I. H., Kerby, J. T., Phoenix, G. K., Bjerke, J. W., Epstein, H. E., Assmann, J. J.,](#)  
1133 [John, C., Andreu-Hayles, L., Angers-Blondin, S., Beck, P. S. A., Berner, L. T., Bhatt, U. S.,](#)  
1134 [Bjorkman, A. D., Blok, D., Bryn, A., Christiansen, C. T., Cornelissen, J. H. C., Cunliffe, A. M.,](#)  
1135 [Elmendorf, S. C., Forbes, B. C., Goetz, S. J., Hollister, R. D., de Jong, R., Loranty, M. M.,](#)  
1136 [Macias-Fauria, M., Maseyk, K., Normand, S., Olofsson, J., Parker, T. C., Parmentier, F. J. W.,](#)  
1137 [Post, E., Schaepman-Strub, G., Stordal, F., Sullivan, P. F., Thomas, H. J. D., Tommervik, H.,](#)  
1138 [Treharne, R., Tweedie, C. E., Walker, D. A., Wilmking, M., and Wipf, S.: Complexity revealed in](#)  
1139 [the greening of the Arctic, \*Nature Climate Change\*, 10, 106-117, doi: 10.1038/s41558-019-0688-](#)  
1140 [1, 2020.](#)

1141 [Naiman, R. J., Melillo, J. M., and Hobbie, J. E.: Ecosystem Alteration of Boreal Forest Streams](#)  
1142 [by Beaver \(\*Castor-Canadensis\*\), \*Ecology\*, 67, 1254-1269, doi: 10.2307/1938681, 1986.](#)

1143 [Nitzbon, J., Westermann, S., Langer, M., Martin, L. C. P., Strauss, J., Laboor, S., and BOike, J.:](#)  
1144 [Fast response of cold ice-rich permafrost in northeast Siberia to a warming climate, \*Nature\*](#)  
1145 [Communications, 11, 2201, doi: 10.1038/s41467-020-15725-8, 2020.](#)

1146 [Nitze, I. and Grosse, G.: Detection of landscape dynamics in the Arctic Lena Delta with](#)  
1147 [temporally dense Landsat time-series stacks, \*Remote Sensing of Environment\*, 181, 27-41, doi:](#)  
1148 [10.1016/j.rse.2016.03.038, 2016.](#)

1149 [Obu, J., Westermann, S., Barboux, C., Bartsch, A., Delaloye, R., Grosse, G., Heim, B.,](#)  
1150 [Hugelius, G., Irrgang, A., Kääb, A. M., Kroisleitner, C., Matthes, H., Nitze, I., Pellet, C., Seifert,](#)  
1151 [F. M., Strozzi, T., Wegmüller, U., Wiczorek, M., and Wiesmann, A.: ESA permafrost Climate](#)  
1152 [Change Initiative \(permafrost\\_cci\): Permafrost extent for the Northern Hemisphere, v2.0](#)  
1153 [\[dataset\], <https://doi.org/10.5285/28E889210F884B469D7168FDE4B4E54F>, 2020.](#)

1154 [Overeem, I., Nienhuis, J. H., and Piliouras, A.: Ice-dominated Arctic deltas, \*Nature Reviews\*](#)  
1155 [Earth & Environment, 3, 225-240, doi: 10.1038/s43017-022-00268-x, 2022.](#)

1156 [Overland, J., Dunlea, E., Box, J. E., Corell, R., Forsius, M., Kattsov, V., Olseng, M. S., Pawlak,](#)  
1157 [J., Reiersen, L. O., and Wang, M. Y.: The urgency of Arctic change, \*Polar Science\*, 21, 6-13,](#)  
1158 [doi: 10.1016/j.polar.2018.11.008, 2019.](#)

1159 [Pickett, S. T. A., Kolasa, J., Armesto, J. J., and Collins, S. L.: The Ecological Concept of](#)  
1160 [Disturbance and Its Expression at Various Hierarchical Levels, \*Oikos\*, 54, 129-136, doi:](#)  
1161 [10.2307/3565258, 1989.](#)

1162 [Piliouras, A. and Rowland, J. C.: Arctic River Delta Morphologic Variability and Implications for](#)  
1163 [Riverine Fluxes to the Coast, Journal of Geophysical Research-Earth Surface, 125, ARTN](#)  
1164 [e2019JF005250, doi: 10.1029/2019JF005250, 2020.](#)

1165 [Pisaric, M. F. J., Thienpont, J. R., Kokelj, S. V., Nesbitt, H., Lantz, T. C., Solomon, S., and Smol,](#)  
1166 [J. P.: Impacts of a recent storm surge on an Arctic delta ecosystem examined in the context of](#)  
1167 [the last millennium, Proceedings of the National Academy of Sciences of the United States of](#)  
1168 [America, 108, 8960-8965, doi: 10.1073/pnas.1018527108, 2011.](#)

1169 [Raynolds, M. K., Walker, D. A., Balser, A., Bay, C., Campbell, M., Cherosov, M. M., Daniels, F.,](#)  
1170 [J. A., Eidesen, P. B., Emiokhina, K. A., Frost, G. V., Jedrzejek, B., Jorgenson, M. T., Kennedy,](#)  
1171 [B. E., Kholod, S. S., Lavrinenko, I. A., Lavrinenko, O. V., Magnusson, B., Matveyeva, N. V.,](#)  
1172 [Metusalemsson, S., Nilsen, L., Olthof, I., Pospelov, I. N., Pospelova, E. B., Pouliot, D.,](#)  
1173 [Razzhivin, V., Schaepman-Strub, G., Sibik, J., Telyatnikov, M. Y., and Troeva, E.: A raster](#)  
1174 [version of the Circumpolar Arctic Vegetation Map \(CAVM\), Remote Sensing of Environment,](#)  
1175 [232, ARTN 111297, doi: 10.1016/j.rse.2019.111297, 2019.](#)

1176 [Romanovskii, N. N. and Hubberten, H. W.: Results of permafrost modelling of the lowlands and](#)  
1177 [shelf of the Laptev Sea region, Russia, Permafrost and Periglacial Processes, 12, 191-202, doi:](#)  
1178 [10.1002/ppp.387, 2001.](#)

1179 [Rossger, N., Sachs, T., Wille, C., Boike, J., and Kutzbach, L.: Seasonal increase of methane](#)  
1180 [emissions linked to warming in Siberian tundra, Nature Climate Change, 12, 1031-+, doi:](#)  
1181 [10.1038/s41558-022-01512-4, 2022.](#)

1182 [Runge, A., Fuchs, M., Shevtsova, I., Landgraf, N., Heim, B., Herzsuh, U., and Grosse, G.:](#)  
1183 [Hyperspectral field spectrometry of Arctic vegetation units in the central Lena Delta \[dataset\],](#)  
1184 [https://doi.org/10.1594/PANGAEA.945982, 2022.](#)

1185 [Sachs, T., Wille, C., Boike, J., and Kutzbach, L.: Environmental controls on ecosystem-scale](#)  
1186 [CH4 emission from polygonal tundra in the Lena River Delta, Siberia, Journal of Geophysical](#)  
1187 [Research-Biogeosciences, 113, Artn G00a03, doi: 10.1029/2007jg000505, 2008.](#)

1188 [Schirrmeister, L., Grosse, G., Schwamborn, G., Andreev, A. A., Meyer, H., Kunitsky, V. V.,](#)  
1189 [Kuznetsova, T. V., Dorozhkina, M. V., Pavlova, E. Y., Bobrov, A. A., and Oezen, D.: Late](#)  
1190 [Quaternary History of the Accumulation Plain North of the Chekanovsky Ridge \(Lena Delta,](#)

1191 [Russia\): A Multidisciplinary Approach, Polar Geography, 27, 277-319, doi: 10.1080/789610225,](#)  
1192 [2003.](#)

1193 [Schirrmeister, L., Grosse, G., Schnelle, M., Fuchs, M., Krbetschek, M., Ulrich, M., Kunitsky, V.,](#)  
1194 [Grigoriev, M., Andreev, A., Kienast, F., Meyer, H., Babiy, O., Klimova, I., Bobrov, A., Wetterich,](#)  
1195 [S., and Schwamborn, G.: Late Quaternary paleoenvironmental records from the western Lena](#)  
1196 [Delta, Arctic Siberia, Palaeogeography Palaeoclimatology Palaeoecology, 299, 175-196, doi:](#)  
1197 [10.1016/j.palaeo.2010.10.045, 2011.](#)

1198 [Schneider, J., Grosse, G., and Wagner, D.: Land cover classification of tundra environments in](#)  
1199 [the Arctic Lena Delta based on Landsat 7 ETM+ data and its application for upscaling of](#)  
1200 [methane emissions, Remote Sensing of Environment, 113, 380-391, doi:](#)  
1201 [10.1016/j.rse.2008.10.013, 2009.](#)

1202 [Schwamborn, G., Rachold, V., and Grigoriev, M. N.: Late Quaternary sedimentation history of](#)  
1203 [the Lena Delta, Quaternary International, 89, 119-134, doi: 10.1016/S1040-6182\(01\)00084-2,](#)  
1204 [2002.](#)

1205 [Schwamborn, G., Schirrmeister, L., Mohammadi, A., Meyer, H., Kartoziia, A., Maggioni, F., and](#)  
1206 [Strauss, J.: Fluvial and permafrost history of the lower Lena River, north-eastern Siberia, over](#)  
1207 [late Quaternary time, Sedimentology, 70, 235-258, doi: 10.1111/sed.13037, 2023.](#)

1208 [Serreze, M. C. and Barry, R. G.: Processes and impacts of Arctic amplification: A research](#)  
1209 [synthesis, Global and Planetary Change, 77, 85-96, doi: 10.1016/j.gloplacha.2011.03.004,](#)  
1210 [2011.](#)

1211 [Shevtsova, I., Laschinskiy, N., Heim, B., and Herzs Schuh, U.: Foliage projective cover of 26](#)  
1212 [vegetation sites of central Lena Delta from 2018 \[dataset\],](#)  
1213 [https://doi.pangaea.de/10.1594/PANGAEA.935875, 2021a.](https://doi.pangaea.de/10.1594/PANGAEA.935875)

1214 [Shevtsova, I., Heim, B., Runge, A., Fuchs, M., Melchert, J., and Herzs Schuh, U.: Total above-](#)  
1215 [ground biomass of 25 vegetation sites of central Lena Delta from 2018 \[dataset\],](#)  
1216 [https://doi.pangaea.de/10.1594/PANGAEA.935923, 2021b.](https://doi.pangaea.de/10.1594/PANGAEA.935923)

1217 [Stanford, J. A., Lorang, M. S., and Hauer, F. R.: The shifting habitat mosaic of river ecosystems,](#)  
1218 [SIL Proceedings, 1922-2010, 29, 123-136, doi: 10.1080/03680770.2005.11901979, 2005.](#)

1219 [Sweeney, C., Chatterjee, A., Wolter, S., McKain, K., Bogue, R., Conley, S., Newberger, T., Hu,](#)  
1220 [L., Ott, L., Poulter, B., Schiferl, L., Weir, B., Zhang, Z., and Miller, C. E.: Using atmospheric](#)  
1221 [trace gas vertical profiles to evaluate model fluxes: a case study of Arctic-CAP observations and](#)  
1222 [GEOS simulations for the ABoVE domain, Atmospheric Chemistry and Physics, 22, 6347-6364,](#)  
1223 [doi: 10.5194/acp-22-6347-2022, 2022.](#)

1224 [Ulrich, M., Grosse, G., Chabrilat, S., and Schirrmeister, L.: Spectral characterization of](#)  
1225 [periglacial surfaces and geomorphological units in the Arctic Lena Delta using field spectrometry](#)  
1226 [and remote sensing, Remote Sensing of Environment, 113, 1220-1235, doi:](#)  
1227 [10.1016/j.rse.2009.02.009, 2009.](#)

1228 [van Everdingen, R. O.: Multi-language glossary of permafrost and related ground-ice terms,](#)  
1229 [Arctic Institute of North America University of Calgary, Calgary, Canada1998.](#)

1230 [Veremeeva, A. and Gubin, S.: Modern Tundra Landscapes of the Kolyma Lowland and their](#)  
1231 [Evolution in the Holocene, Permafrost and Periglacial Processes, 20, 399-406, doi:](#)  
1232 [10.1002/ppp.674, 2009.](#)

1233 [Vulis, L., Tejedor, A., Zaliapin, I., Rowland, J. C., and Foufoula-Georgiou, E.: Climate](#)  
1234 [Signatures on Lake And Wetland Size Distributions in Arctic Deltas, Geophysical Research](#)  
1235 [Letters, 48, ARTN e2021GL094437, doi: 10.1029/2021GL094437, 2021.](#)

1236 [Walker, H. J.: Arctic deltas, Journal of Coastal Research, 14, 718–738, 1998.](#)

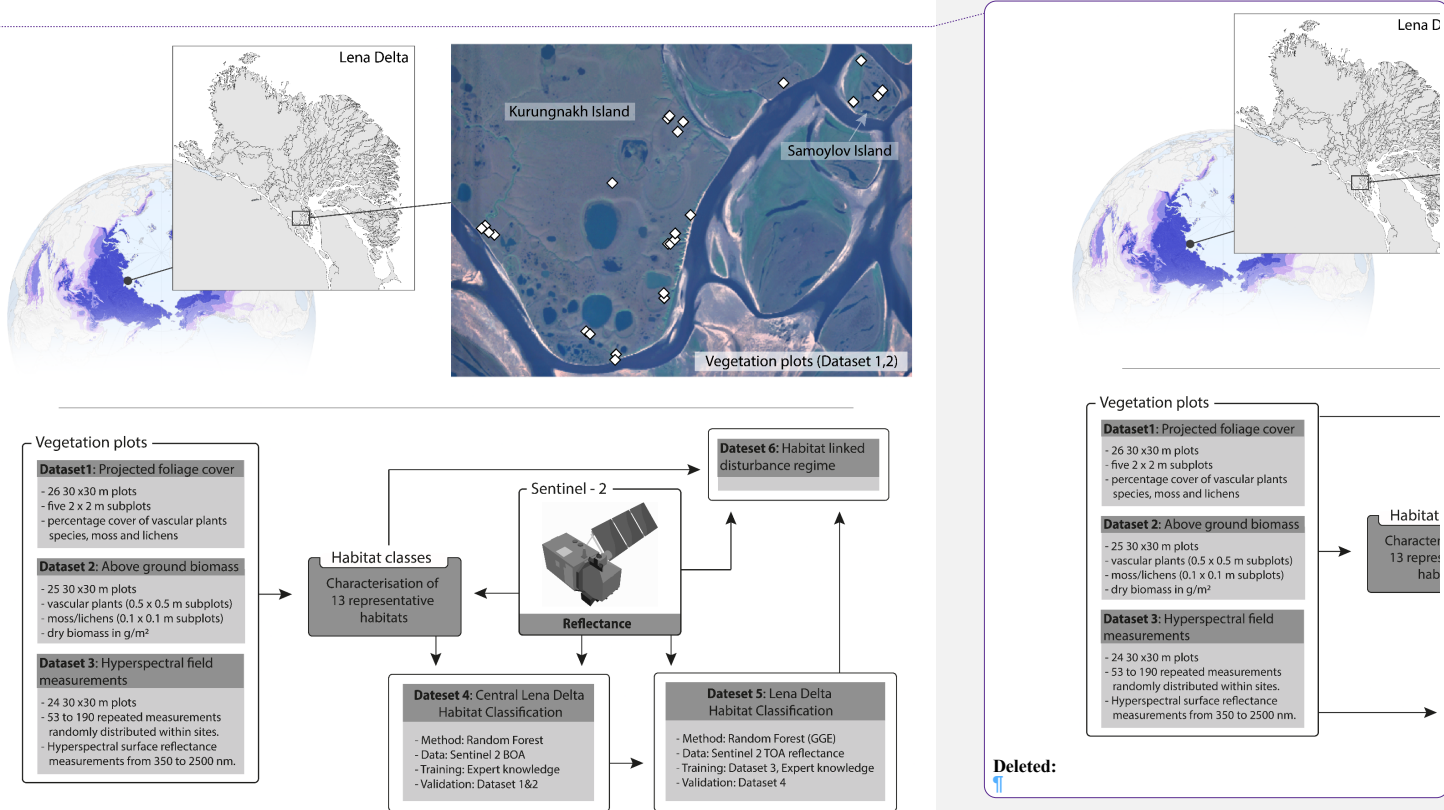
1237 [Whitaker, R. H. and Woodwell, G. M.: Dimension, and Production Relations of Trees and](#)  
1238 [Shrubs in the Brookhaven Forest, New York., Journal of Ecology, 56, 1-25, doi: 10.1038/2325,](#)  
1239 [1968.](#)

1240 [Zibulski, R., Herzsuh, U., and Pestryakova, L. A.: Vegetation patterns along micro-relief and](#)  
1241 [vegetation type transects in polygonal landscapes of the Siberian Arctic, Journal of Vegetation](#)  
1242 [Science, 27, 377-386, doi: 10.1111/jvs.12356, 2016.](#)

1243

1244 **Figures**

1245



1246

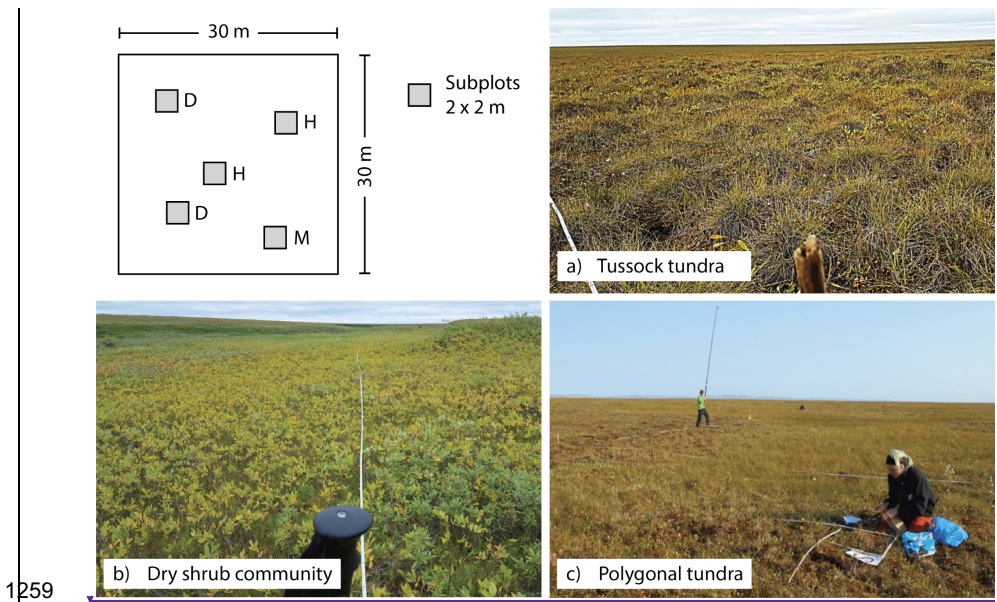
1247 **Figure 1:** Geographic location of the Lena Delta in the Russian High Arctic (72.91°N, 126.90°E)  
 1248 and a Sentinel-2 RGB image (August 2018, bands 4-3-2) of the central Lena Delta showing the  
 1249 areas of the 26 vegetation plots where foliage projective cover and above ground biomass was  
 1250 determined. Panarctic overview map shows permafrost extent (colour scale indicates  
 1251 permafrost extent from continuous (dark purple) to isolated (light purple) (Obu et al., 2020). The  
 1252 grey-coloured Lena Delta land map created with Sentinel-1 water mask from Juhls et al. (2021).  
 1253 Bottom: Dataset characteristics and methodological links between the different datasets.

Deleted:

Deleted: :

Deleted: .

Deleted: .

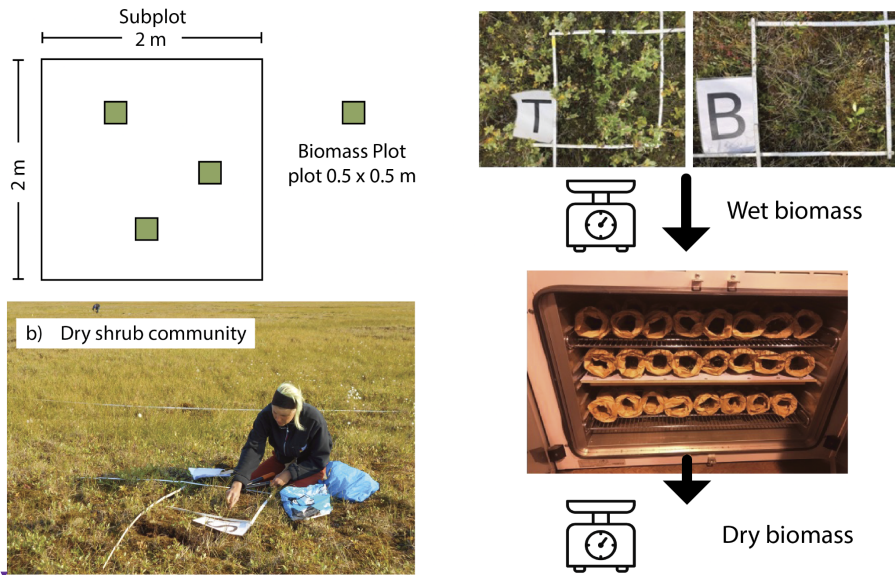


1259  
 1260 Figure 2. Vegetation plots (30 x 30 m) were established in different vegetation types across the  
 1261 central Lena Delta. For subplots (2 x 2 m), the projective vegetation cover was recorded and  
 1262 labeled according to vegetation and moisture properties (H-Type: homogeneous, M-Type:  
 1263 moist, D-Type: dry). Figures illustrate example plots in a) tussock tundra (VP14), b) dry shrub  
 1264 communities (VP05), c) polygonal tundra (VP13). Photos: AWI.

Deleted: .....Page Break.....

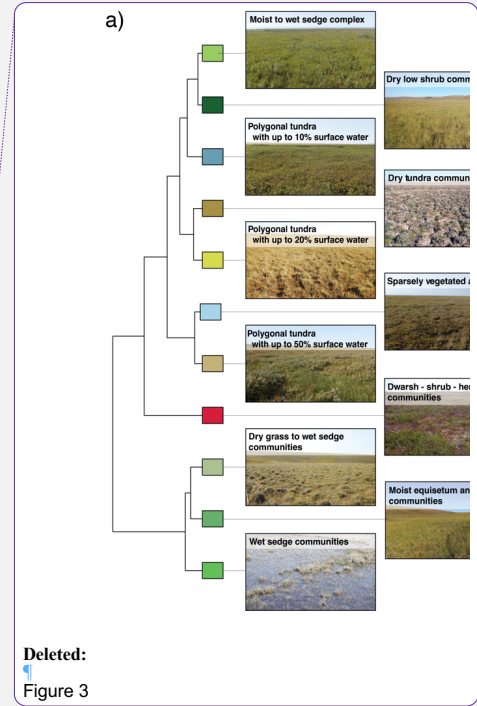
Taxa	Cover, %	Height, cm
all	100	
Salix pulchra	20	10-12
Bistorta vivipara	0.5	
Carex concolor	1	13
Dryas punctata	0.5	
Saxifraga aestivalis	0.5	
Pedicularis albolabiata	0.5	
moss	88	
lichen	2	

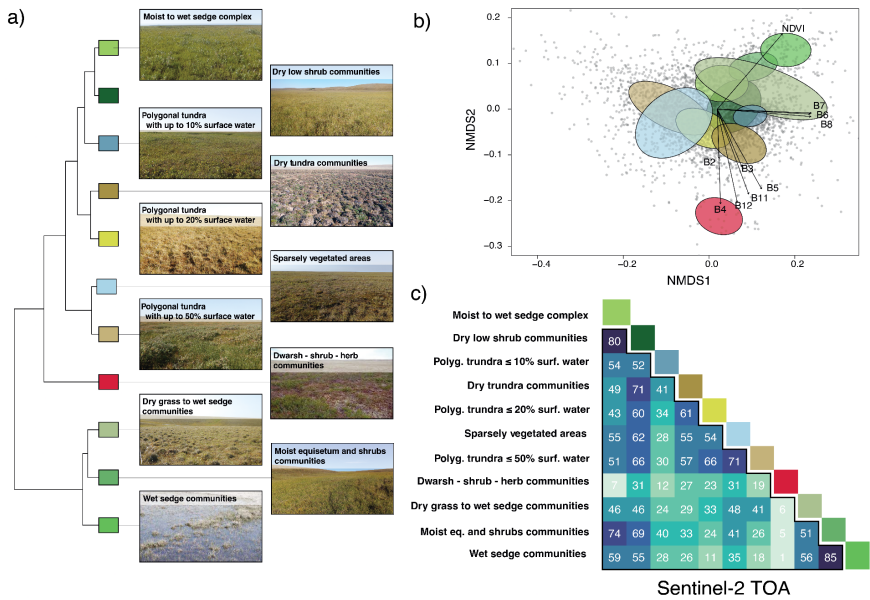
- Deleted: : Schematic
- Deleted: plot set up with 2 x 2 m
- Deleted: for
- Deleted: estimation for different canopy layers
- Deleted: above ground biomass sampling on 0.5 x 0.5m inside the 2 x 2 m subplots. The background photo shows a...
- Deleted: plot within the
- Deleted: , a relatively homogenous vegetation class that would account for one class only. Schematically we here added green and red polygons that would define sub-vegetation classes, e.g., with different moisture regimes)....



1282

1283 Figure 3. Biomass was sampled in subplots of 0.5 x 0.5 m (and 0.1 x 0.1 m for moss and  
 1284 lichens) distributed within the 2 x 2 m subplots described in Figure 2. Collected plants were  
 1285 weighted (wet biomass), dried in an oven and again weighted (dry biomass). Fotos: AWI.

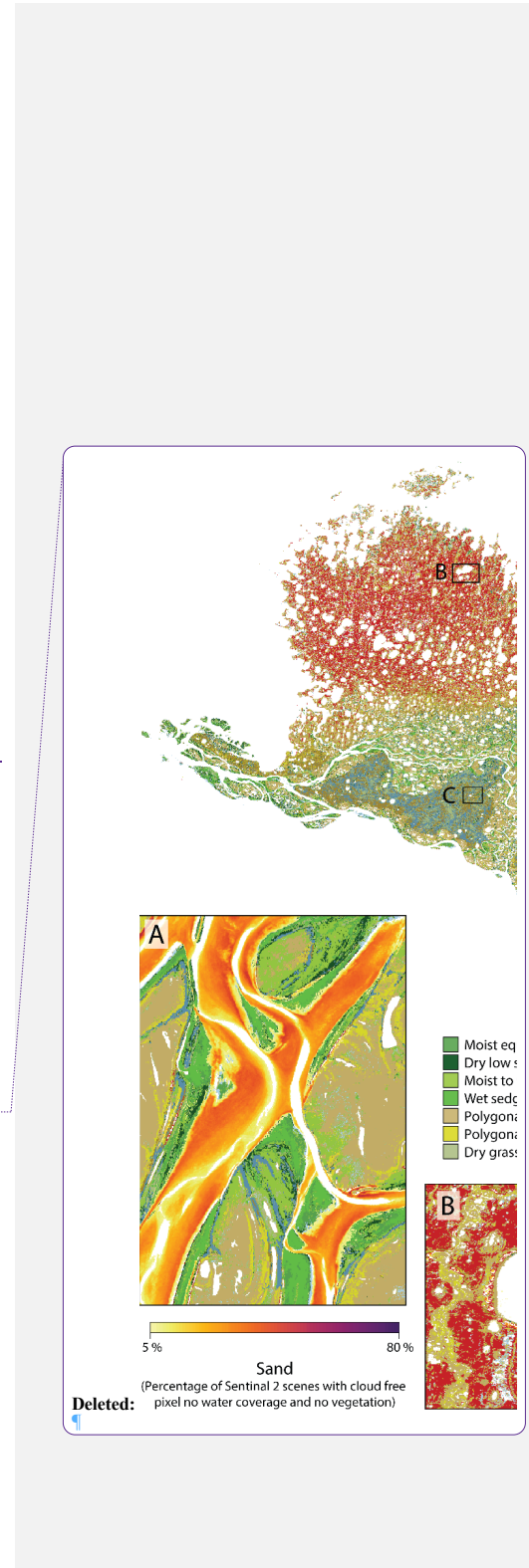


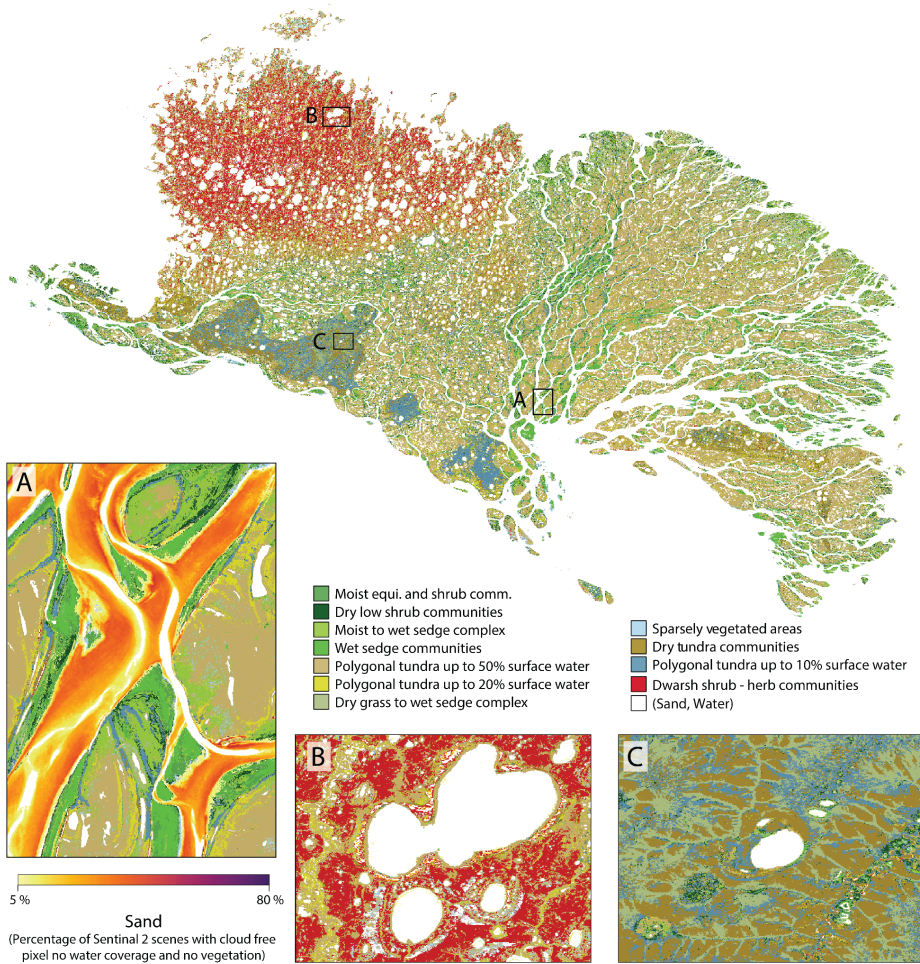


1289

1290 **Figure 4:** Similarity of habitat classes based on Sentinel-2 spectral reflectance and NDVI values.  
 1291 The dendrogram in panel a) indicates the multidimensional hierarchical similarity of the classes  
 1292 based on Sentinel-2 top of atmosphere reflectance (bands 2-8, 10-12, and NDVI). Panel b)  
 1293 shows the location of the habitat classes within a two-dimensional NMDS space. The arrows  
 1294 with the Sentinel-2 bands and NDVI indicate the correlation of these variables across the two  
 1295 axes. The lower matrix of panel c) depicts the calculated percentage overlap of 3,500 pixels  
 1296 (grey dots in panel b) across the two NMDS axes of panel b).

1297





1300

1301

1302

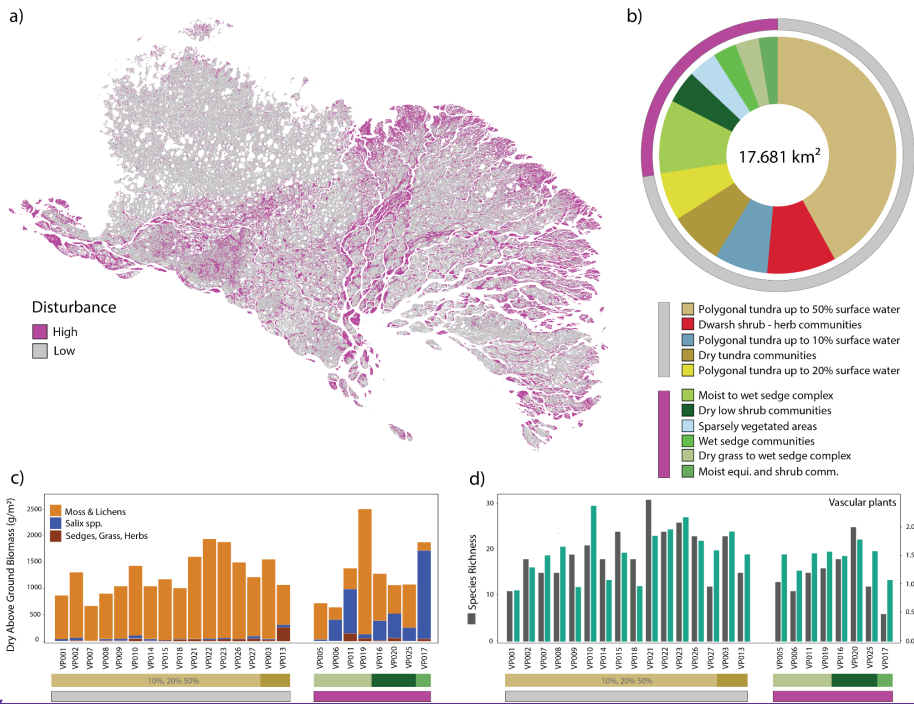
1303

Figure 5: Lena Delta habitat classes (Dataset 5). The entire Lena Delta on the left with three regional examples, showing (A) the seasonal sand probability and (B, C) regional examples of the habitat classes.

Deleted: 4

Deleted: ,B,C) includes

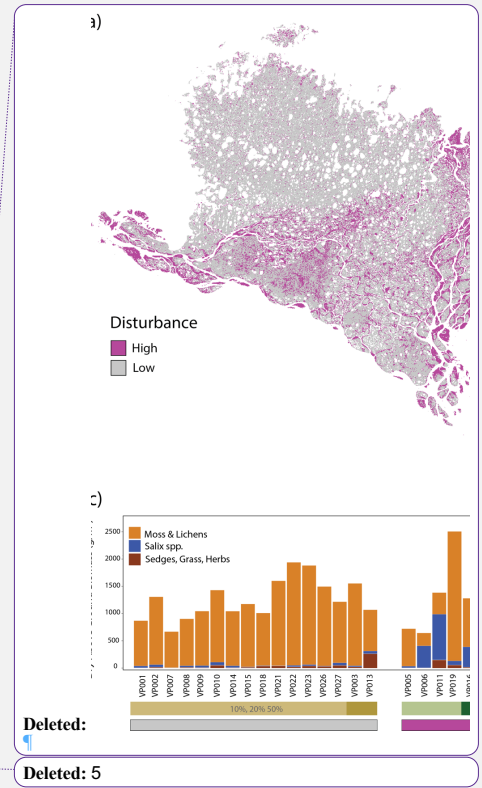
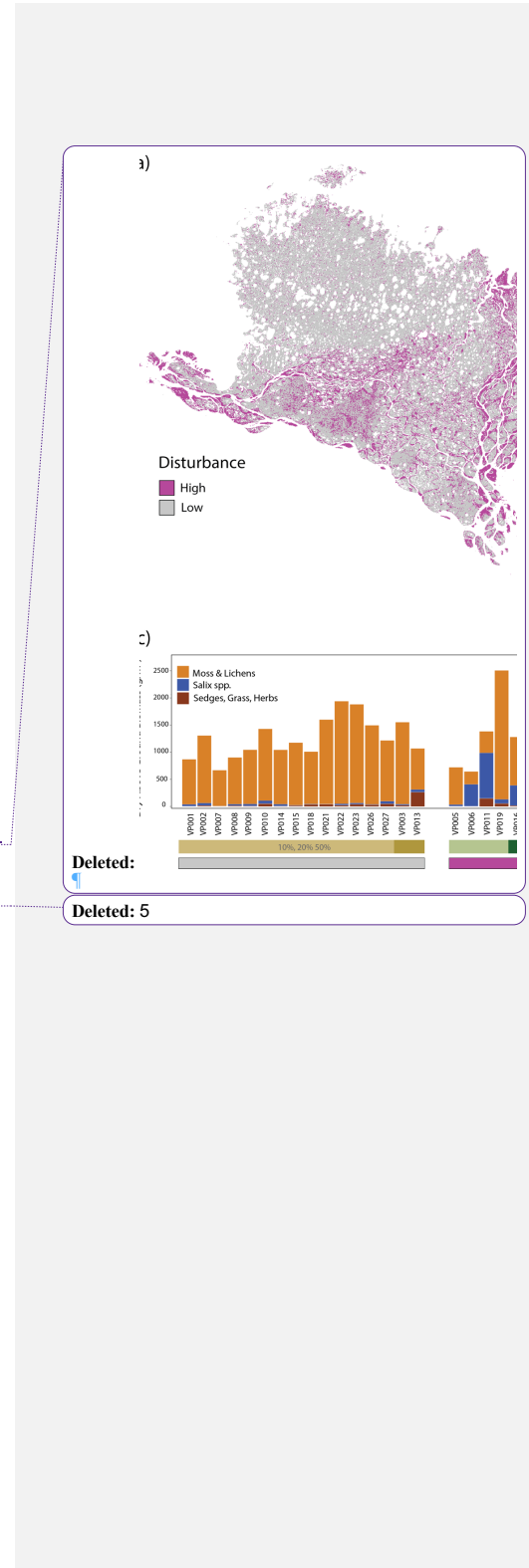
Deleted: map



1307

1308 **Figure 6:** Habitat linked disturbance regimes across the Lena Delta. The map (a) includes all  
 1309 vegetated areas (excluding water and sand). The pie chart (b) shows the contribution of  
 1310 vegetated classes across the Lena Delta grouped by high and low disturbance regimes. The  
 1311 bottom panels show c) the measured dry above ground biomass (Dataset 2) and d) the species  
 1312 richness and Shannon index (from Dataset 1) of the vegetation plots for different habitat classes  
 1313 and disturbance regimes.

1314



Deleted:

Deleted: 5

1318 **Tables**

1319 Table 1: Habitat classes, descriptions as well as methods used to characterize the distinct  
 1320 habitats. In-situ vegetation plot numbers correspond to the vegetation plots of Dataset 1 and 2  
 1321 (see also Table S1, S2, S3).

Deleted: types

1322

Habitat types	Description	Method
<b>Moist <i>Equisetum</i> and shrubs</b>	<i>Equisetum</i> and shrub communities form a early-to-middle successional stage growing on the active floodplain. Low moss contribution	In-situ vegetation plot (VP17); extended to representative larger polygon shape files using field knowledge.
<b>Dry shrub communities</b>	Patch forming shrub communities dominated by dwarf willow ( <i>Salix</i> ) thickets, frequently occurring on dry elevated areas on floodplains and stream floodplains and in topographically sheltered areas below basin and valley rims. Low moss contribution	In-situ vegetation plots (VP04, VP16); extended to representative larger polygon shape files using field knowledge.
<b>Polygonal tundra complex</b>  up to - 10% - 20% - 50% surface water  (3 distinct classes)	Mature-state plant communities dominated by sedge, moss and herb species. Sparse vascular plant coverage (dwarf willows, dwarf birches) on thick continuous moss cover. Occurring on the plateaus of the ice-rich holocene and pleistocene terraces, and at the bottom of alases. Intersected by intra- and interpolygonal ponds resulting in up to 10%, 20%, 50% surface water contribution.	In-situ vegetation plots (VP01, VP02, VP07, VP08, VP14, VP15, VP18, VP21, VP22, VP23, VP26, VP27); extended to representative larger polygon shape files using field knowledge. The different surface water contributions were defined based on the result from unsupervised classification.

<p><b>Dry grass to wet sedge communities</b></p>	<p>These early-to-middle successional plant communities cover unstable valley slopes and a <del>young drained</del> lake basin, they are mostly composed of sedges and grasses, but also willows (<i>Salix</i>) are part of this habitat.</p>	<p>In-situ vegetation plots (VP05, VP06, VP11, VP19, VP20); extended to representative larger polygon shape files using field knowledge.</p>
<p><b>Dry tundra communities</b></p>	<p>The mature-state dry tundra communities represent the zonal tundra type, one subclass is dominated by tussock forming <i>Eriophorum</i> and the other by less tussock forming dry-herb communities, dominated by <i>Dryas</i>. Occurring on well-drained slopes of valleys and alases, and other well-drained areas on the terraces. High moss contribution</p>	<p>In-situ vegetation plots (VP03, VP13) extended to representative, larger polygon shape files using field knowledge (including 'dry tundra communities type tussock' and 'dry tundra communities').</p>
<p><b>Moist to wet sedge communities</b></p>	<p>These mid to advanced successional plant communities occur on moist to water-logged soils characteristically mostly in topographic depressions on the floodplains, in valleys and alases. They constitute the rims of the wetland areas on the floodplains in more dynamic parts the moss ground cover is missing.</p>	<p>Polygon shape files derived from high resolution satellite image and ESRI GE with regional expert knowledge. No vegetation plots (too wet).</p>
<p><b>Wet sedge communities</b></p>	<p>These mid to advanced successional plant communities occur at permanently wet sites with stagnant water in the topographic depressions and are typical for wetland areas on the floodplains. In more dynamic parts the moss ground cover is missing.</p>	<p>Polygon shape files derived from high resolution satellite image and ESRI GE with regional expert knowledge. No vegetation plots (too wet).</p>

Deleted: young drained

<b>Sparse vegetated areas</b>	These early successional plant communities are characterized by low vegetation establishment and coverage. No to low moss contribution	Defined based on the result from unsupervised classification, polygon shape files. No vegetation plots.
<b>Barren/Sand</b>	Representing the wide-open sand flats of the floodplain and barren ground on valley slopes or along cliffs. In a few cases, this class represents vegetation-free bedrock outcrops.	Threshold using high reflectance in S2-band 2 blue.
<b>Water</b>	Represents all surface water bodies in the delta: the Lena River with river branches, streams, lakes and large ponds.	Threshold using low reflectance in S2-band 8 NIR.

1325

1326 Table 2: Habitat class and description of disturbance regimes and the component stand  
 1327 structure in form of contributions of vascular plants, and moss to total biomass. \* (Driscoll and  
 1328 Hauer, 2019; Stanford et al., 2005), \*\* (Lorang and Hauer, 2006).

Deleted: \*, \*\*.

Habitat class	Disturbance regime	Stand structure
<b>Moist <i>Equisetum</i> and shrubs</b>	<b>High; regular (annually), predicted</b> - spring floodings, - shifting habitat * - advanced-stage regeneration **	high vascular plant growth, low abundance of moss & lichens.
<b>Dry shrub communities</b>	<b>High; mixed disturbance types:</b> -regular spring floodings -rapid thaw processes (permafrost degradation) - shifting habitat - advanced-stage regeneration	high vascular plant growth, low abundance of moss.
<b>Polygonal tundra complex</b>	<b>Low; mixed disturbance types</b> - low for most of the habitat, except for actively eroding shores of ponds and channels - mature-state plant community	low vascular plant growth, high abundance of moss.
<b>Dry grass to wet sedge communities</b>	<b>High; mixed disturbance types:</b> - regular spring floodings - rapid thaw processes (permafrost degradation) - shifting habitat	high vascular plant biomass, low abundance of moss.

	- advanced-stage regeneration	
<b>Dry tundra communities</b>	<b>Low; mixed disturbance types</b> - low for most of the habitat - mature-state plant community	low vascular plant biomass high abundance of moss.
<b>Moist to wet sedge communities</b>	<b>High; mixed disturbance types:</b> - regular spring floodings - rapid thaw processes (permafrost degradation) - shifting habitat - mid to advanced-stage regeneration	high vascular plant biomass Almost impossible to measure in-situ biomass (wet conditions and difficult access).
<b>Wet sedge communities</b>	<b>High; mixed disturbance types:</b> - regular spring floodings - rapid thaw processes (permafrost degradation) - shifting habitat - mid to advanced-stage regeneration	high vascular plant biomass. Almost impossible to measure in-situ biomass (wet conditions and difficult access).
<b>Dwarf shrub herb communities</b>	<b>Low; mixed disturbance types</b> - low for most of the habitat - mature-state plant community	low vascular plant biomass, high abundance of moss.

<p><b>Sparsely vegetated areas</b></p>	<p><b>Very high; mixed disturbance types</b></p> <ul style="list-style-type: none"> <li>- regular spring floodings</li> <li>- rapid thaw processes (permafrost degradation)</li> <li>- shifting habitat</li> <li>- early-stage regeneration</li> </ul>	<p>lowest vascular plant biomass, no moss.</p>
<p><b>Sand banks/barren</b></p>	<p><b>Very high: mixed disturbance types</b></p> <ul style="list-style-type: none"> <li>- regular spring floodings</li> <li>- rapid thaw processes (permafrost degradation)</li> <li>- shifting habitat</li> <li>- no regeneration</li> </ul>	<p>Barren, constant shifting of sediments and movement of soils.</p>

1330